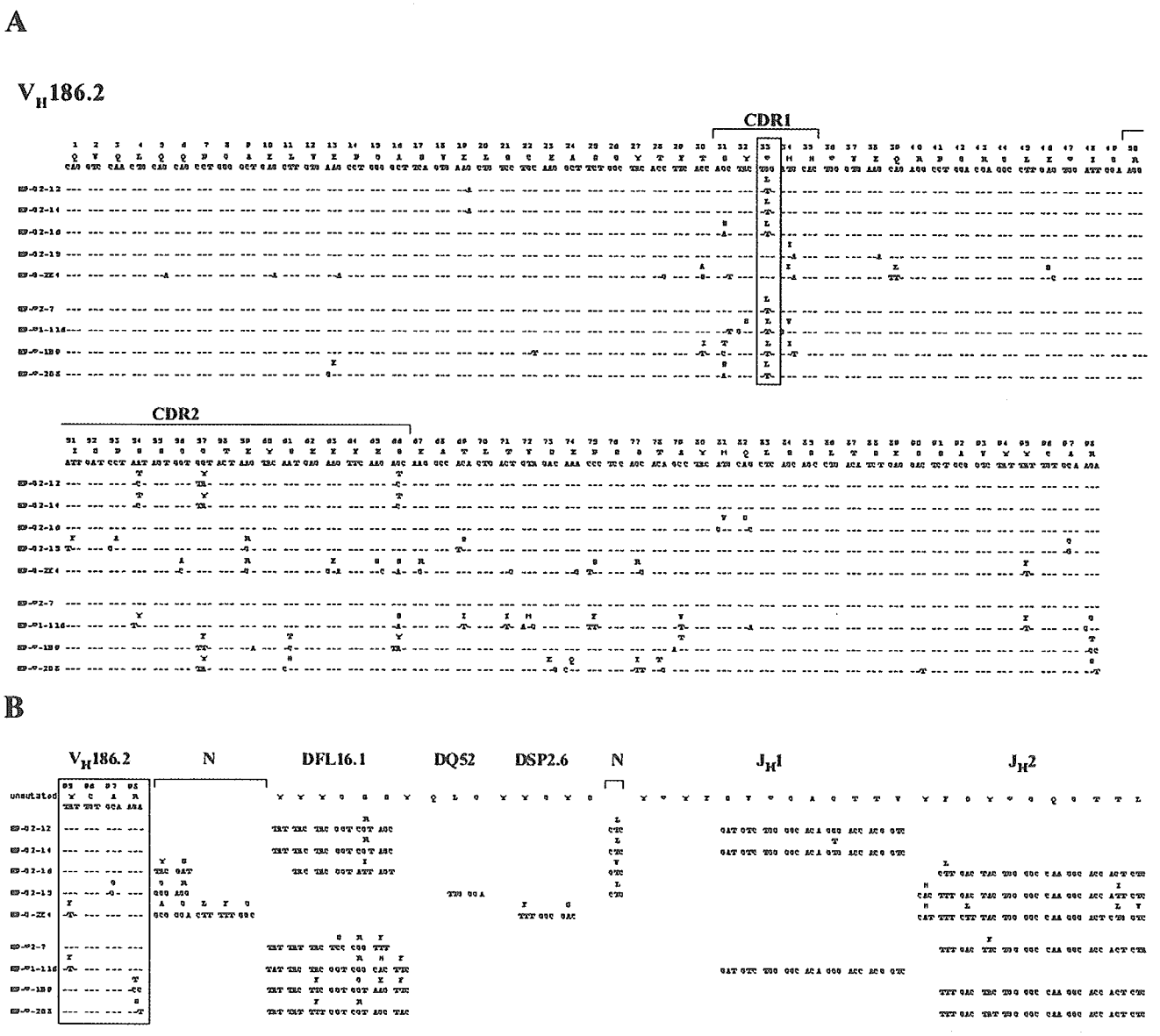

FIGURE 2. *(continues)*

We examined whether *Ganp*^{Tg} mice showed the alteration of GC formation in vivo. *Ganp*^{Tg} mice did not show any difference in the size and number of GCs at day 10 after SRBC immunization; however, in contrast to the findings observed in B-*ganp*$^{-/-}$ mice (4), *Ganp*^{Tg} mice showed the accelerated resolution of GC formation in vivo (Fig. 1*F*). This response could be due to the efficient production of high-affinity Ab in *Ganp*^{Tg} mice.

Responses of Ganp^{Tg} *mice against T cell-independent Ag and TD-Ag*

Because GANP expression is selectively up-regulated in GC B cells, we studied the Ab responses of *Ganp*^{Tg} mice. After Ag immunization, the responses were measured for T cell-independent type II Ag and TD-Ag at various time points and the results of day 14 were shown. The serum titers of Ag-specific Abs against TNP-Ficoll as T cell-independent Ag and TNP-KLH as TD-Ag were normal with similar distributions of various Ig isotypes in comparison with wild-type littermates (Fig. 1*G*).

Enhanced affinity maturation of Ganp^{Tg} *mice against TD-Ag*

However, after immunization with NP-CG, *Ganp*^{Tg} showed high affinity by the differential ELISA with the pauci NP_2-BSA conjugate that yielded 42% of the response to the multihapten NP_{17}-BSA conjugate in comparison with C57BL/6 (Fig. 1*H*). Jacob et al. (15, 16) showed that, in (NP-CG)-immunized C57BL/6 mice, the Abs in the secondary response against NP were exclusively IgG1/λ1 and had a single V_H region (V_H186.2) carrying with a peculiar pattern of mutation for high affinity. We investigated whether the affinity increase of anti-NP Ab generated in *Ganp*^{Tg} mice accompanied with the similar mutation pattern in the *V_H186.2* locus. The *V_H186.2* sequence was studied by RT-PCR using the spleen B cells from (NP-CG)-immunized mice. *Ganp*^{Tg} showed striking increases in mutation at ^{33}W to L of the *V_H186.2* locus in splenic B cells (W33L; Fig. 1*I*). These results demonstrated that *Ganp*^{Tg} induced a higher frequency of the high-affinity mutation during the immune response to TD-Ag.

Establishment of hybridomas secreting high-affinity anti-NP-hapten

Anti-NP hybridomas were established by immunization of *Ganp*^{Tg} with NP-CG. Supernatants from >6000 clones were screened by the differential ELISA to identify wells with high-affinity mAbs, and the selected hybridoma cells were cloned. Affinities of those

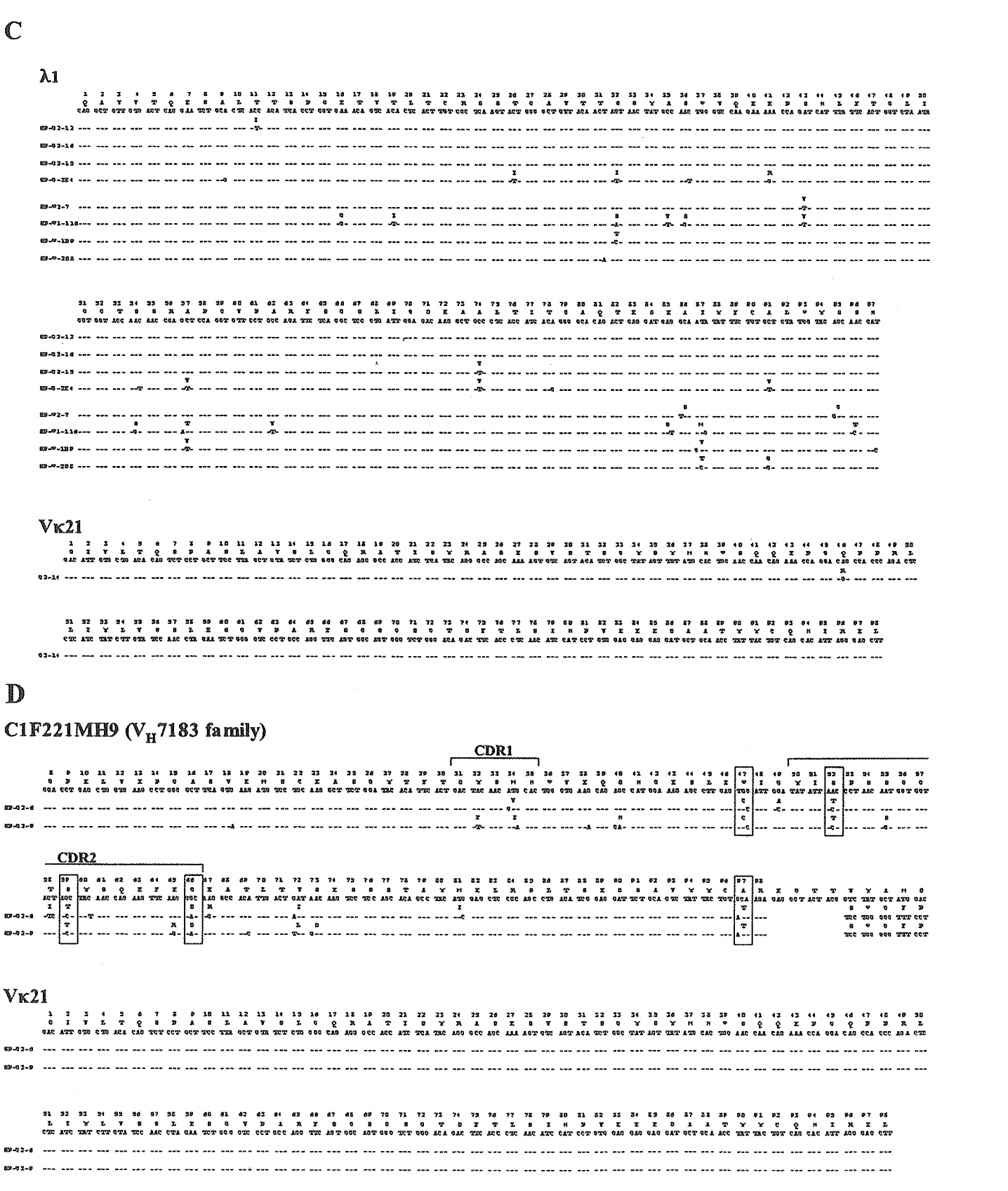

FIGURE 2. Sequence analysis of the *V* region genes of the hybridomas secreting anti-NP mAbs. V_H regions were determined using the primers commonly applicable to the major V_H families and the J_H4 primer (12). The individual *V* region sequence was determined after cloning of the genomic PCR products. Each sequence was determined by three sequencing reactions. *A*, The sequences of the clones using the V_H186.2 region are aligned and the site of W33L mutation is boxed. *B*, The sequences of the VDJ recombination regions are aligned. The part of the V_H186.2 region was boxed. *C*, The V_L region sequences were determined similarly to the method used for V_H regions. *D*, The sequences of the V_H and V_L regions of the two anti-NP mAbs that used noncanonical V_H regions are shown. The mutations shared between the two mAbs are boxed.

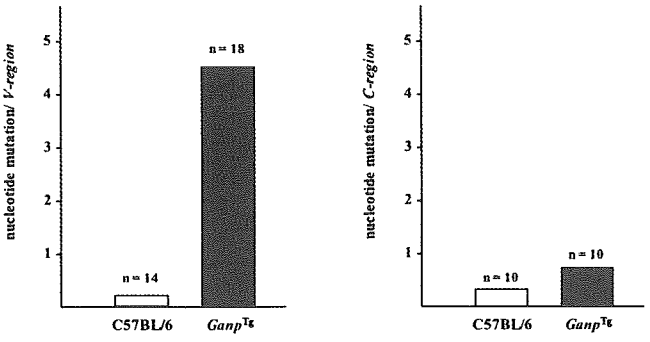

FIGURE 3. Mutation frequency induced in the V_H7183 family gene (C1F221MH9) by NP-CG immunization. NP-binding GC B cells were purified by a cell sorter 14 days after immunization with NP-CG in $Ganp^{Tg}$ and C57BL/6 mice. The V_H7183 family gene and $C\mu$ gene were PCR-amplified by Pfu-Turbo with genomic DNAs, cloned into TOPO cloning vector, and then sequenced. The mutation frequencies were counted based on the genomic sequences in the European Molecular Biology Laboratory database and were shown as average mutations per V_H region or $C\mu$ region sequences. The number (n) shows the V_H region (*left*) or $C\mu$ region (*right*) DNAs cloned in the TOPO cloning vector.

mAbs, after purification from clone culture supernatants, to NP-hapten were measured by the BIAcore system with a sensor chip conjugated with NP using Pharmacia Kinetics Evaluation software (9). The K_D of each mAb was determined by measuring the rate of binding to the Ag at different protein concentrations. The affinity of mAbs from (NP-CG)-immunized $Ganp^{Tg}$ and C57BL/6 mice were compared and the representatives were shown (Table I). The high-affinity mAbs of C57BL/6 mice used the $V_H186.2$ region in combination with λ1 L chain and yielded affinities from $K_D = 1.51 \times 10^{-7}$ M to 1.0×10^{-8} M. The mAbs from $Ganp^{Tg}$ showed the usage of canonical $V_H186.2$ in combination with both κ and λ yielding affinities from $K_D = 1.10 \times 10^{-7}$ M to 1.57×10^{-9} M. Interestingly, the mAbs from $Ganp^{Tg}$ also used noncanonical V_H region of V_H7183 family in combination κ-chain but showed similarly high affinities.

The usage and mutation of V *region genes in the anti-NP hybridomas*

The high-affinity mAbs obtained from C57BL/6 mice used the canonical $V_H186.2$ gene with the W33L mutation that is responsible for high affinity. This change increased the affinity from $K_D = 2 \sim 4 \times 10^{-6}$ M to 2×10^{-7} M (17, 18). The other mutations in the $V_H186.2$ gene segment would not have contributed to increased affinity against NP-hapten (19). Therefore, we sequenced the V_H regions of the hybridomas to examine whether there were similar mutation profiles of the V region. The mAbs from C57BL/6 mice generated typical high affinity against NP-hapten by using the $V_H186.2$ region with W33L mutation in combination with $DFL16.1$ and J_H2 gene segments. $Ganp^{Tg}$ generated similar high-affinity mAbs (NP-G2-12; $K_D = 4.92 \times 10^{-8}$, NP-G2-16; 1.10×10^{-7} M) (Table I) with the V_H186.2 having the W33L mutation (Fig. 2*A*). Interestingly, two anti-NP hybridomas that did not bear the W33L mutation in V_H186.2 showed similar high affinities. NP-G2-15 had the mutation of Y99G as reported previously (10). NP-G-2E4 with higher affinity ($K_D = 1.57 \times 10^{-9}$ M) did not have either of these two mutations but instead showed 13 aa mutations (22 nt changes) in the V_H186.2 region with the usage of DSP2.6 and J_H2 regions (Fig. 2, *A* and *B*). The L chain of NP-G-2E4 also had 6 aa mutations (10 nt changes) (Fig. 2*C*). This result suggested that the high affinity of NP-G-2E4 was generated by the extraordinarily increased V region mutations.

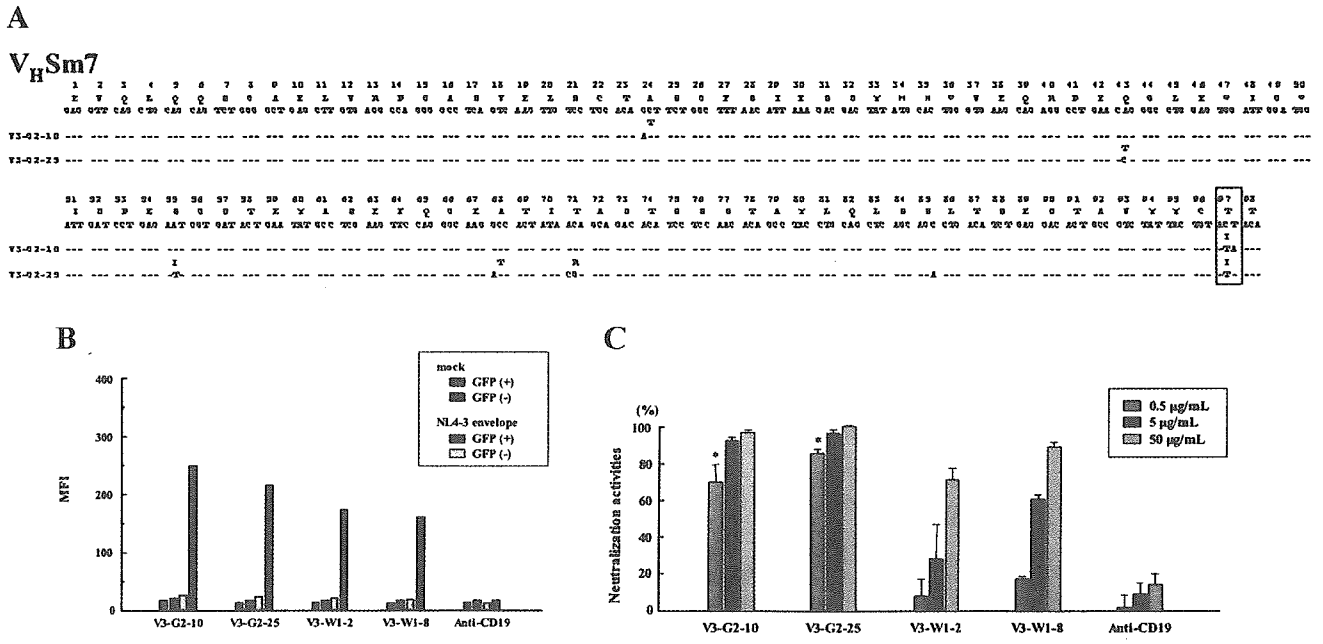

FIGURE 4. The sequences of the V_H region, the Ag-binding activities, and the neutralizing activities of the mAbs against the V3 epitope of HIV-1 gp120. *A*, The V_H region sequence (V_HSm7) used for the high-affinity mAbs from $Ganp^{Tg}$ is shown. The mutation site commonly observed in the two V_H sequences is boxed. *B*, Binding activity of the mAbs against HIV-1 envelope. Specific binding of the mAbs were shown as mean fluorescence intensity (MFI) examined with allophycocyanin-conjugated goat anti-mouse IgG Ab in combination with the NL4-3 envelope-expressing GFP^+-transfectants by using flow cytometry. Negative controls were measured with GFP^--mock transfectants. Another negative control for mAb binding was shown by CD19 mAb. *C*, Neutralizing activities were measured using a CD4-LTR/β-galactosidase-induced HeLa cell line. After $TCID_{50}$ of virus stock was predetermined with MAGI/CCR5 cells, the virus infection assay was conducted in vitro, to which anti-V3 epitope mAbs were added. Higher neutralization activities were significant (*) for the mAbs produced by $Ganp^{Tg}$ (V3-G2-10 and V3-G2-25) as compared with those of C57BL/6 mice at the concentration of 0.5 μg/ml. Negative control is shown with anti-CD19.

Moreover, two anti-NP mAbs from *Ganp*^{Tg} yielding similarly high affinities (K_D = 3.24 ~ 7.05 × 10^{-8} M) used noncanonical V_H region sequences, both of which probably originated from the same genomic *V_H7183* family. The best match in the Celera Discovery System was to the C1F221MH9 (*V_H7183* family), but the two clones showed variations with >12 nt differences from the genomic C1F221MH9 sequence (Fig. 2*D*). Mutations of W47C, N52C, S59T, G66D, and A97T were commonly observed in the V_H region (C1F221MH9), suggesting their contributions to raise the affinity of the mAb against NP-hapten. However, mutations in the V_L regions were not apparently increased in the comparison of the anti-NP mAbs from *Ganp*^{Tg} and C57BL/6 mice. The generation of high-affinity BCR without the exchange at position 33 is a rare event, which suggested that the combination of particular D-J_H sequences and/or many SHMs do not result in high affinity (18). A recent report only showed the case of mutation, Y99G in V_H186.2, which generated similar high-affinity mAb against NP-hapten comparable to W33L (10). Extensive earlier studies of anti-NP mAbs found that repeated immunization of C57BL/6 mice with NP-CG increased usage of noncanonical V_H regions and different L chain combinations (16). However, as far as we know, no study with conventional animals has demonstrated comparable high-affinity mAbs to those reported in this study. Although crystallographic studies are needed for definitive conclusions, we speculate that hypermutated C1F221MH9 V_H region (V_H7183 family) in association with other L chain combinations creates an effective tertiary structure for Ag-binding, yielding closer interactions of hypermutated C1F221MH9 V_H region and NP-hapten, and might be as effective as mAbs with the V_H186.2 region.

Mutations induced in the noncanonical V_H region of the spleen B cells after immunization with NP-CG

Usually wild-type C57BL/6 mice do not induce such a frequent mutation in the noncanonical V_H region in GC B cells before and after immunization with NP-CG. We examined the mutation frequency of the *V_H7183* family gene (C1F221MH9) under a non-immunization condition in spleen B cells of *Ganp*^{Tg} mice but found no alteration of the V_H region (data not shown). To study whether such hypermutation could be observed in *Ganp*^{Tg} spleen B cells after immunization, we investigated mutations in the *V_H7183* family gene (C1F221MH9) by examining genomic DNA of NP-binding GC B cells purified by cell sorting. These DNAs showed 16-fold higher mutation frequencies (4.5 mutations/V_H region of *Ganp*^{Tg} mAb vs 0.28 mutations/V_H region of C57BL/6 mAb) in the *V_H7183* family (Fig. 3, *left panel*). In contrast, such higher mutation frequencies were not observed in the Cμ region (Fig. 3, *right panel*). This is in agreement with the suggestion that *Ganp*^{Tg} has a high frequency of SHM that contributes to the production of high-affinity BCR in vivo. Alternatively, *Ganp*^{Tg} might effectively rescue and maintain B cells with high-affinity BCR during the immune response.

Establishment of high-affinity mAbs against HIV-1 by use of Ganp^{Tg} *mice*

To apply this system for generating high-affinity Ab using *Ganp*^{Tg} mice, we studied whether high-affinity anti-HIV-1 mAbs with significant neutralization activity against virus infection could be generated by immunization with the V3 loop peptide (NL4-3) of HIV-1 gp120. Differential ELISA using plates coated with high and low doses of the V3 peptide initially identified hybridoma cells with relatively high-affinity mAbs from >6000 wells of (V3 peptide)-immunized *Ganp*^{Tg} and C57BL/6 mice. High-affinity clones were selected from each mouse strain. After further cloning, individual mAbs were purified and their affinities were measured using the BIAcore system. The mAbs from both mouse systems showed higher affinities in a range from K_D = 2.81 × 10^{-5} M to ~ 5.67 × 10^{-9} M. However, we could obtain extraordinarily higher affinity mAbs (V3-G2-10 and V3-G2-25; K_D = 9.90 × 10^{-11} M) from *Ganp*^{Tg} over the level that is generally not attainable by conventional methods of mAb preparation (20). The highest affinity mAbs (V3-W1-2 and V3-W1-8) from C57BL/6 mice were up to K_D = 9.81 × 10^{-8} M and 7.58 × 10^{-8} M. The high-affinity mAbs from *Ganp*^{Tg} used the same V_H region (V_HSm7) with the common mutation at T97I, suggesting that the T97I mutation contributed to an affinity increase against the V3 epitope (Fig. 4*A*). A binding assay involving HIV-1 envelope (NL4-3) gene-transfected cells was used to determine whether the mAb recognized the viral epitope. The binding activities to the transfectants were studied by flow cytometry as mean fluorescence intensity in comparison with the GFP-positivity as indicators of gene transfection. The mAbs (V3-G2-10, V3-G2-25, V3-W1-2, and V3-W1-8) showed higher binding activities to the virus epitope-expressing cells (Fig. 4*B*).

The neutralization activities of these anti-HIV-1 mAbs were examined using a CD4-LTR/β-galactosidase-transduced HeLa cell line that expresses high levels of human CD4 and contains a single integrated copy of a *β-galactosidase* gene under the control of a truncated HIV-1 LTR (13, 21). Neutralization activities of the two high-affinity mAbs (V3-G2-10 and V3-G2-25) were clearly detected at 0.5 μg/ml, which were more effective than those of mAbs (V3-W1-2 and V3-W1-8) from C57BL/6 (Fig. 4*C*). The simple comparison might indicate 50–100 times increase of affinity in the mAbs from *Ganp*^{Tg} mice. These mAbs with high-affinity Ag-binding and neutralization activities should be useful for clinical diagnostic purposes and analogous human mAbs might have therapeutic possibilities (22).

Discussion

Expression of GANP is required for generation of high-affinity Ab response in vivo, which was demonstrated by conditional targeting of *ganp* gene in B cells that caused apparent decrease in production of high-affinity Ab against NP-hapten, accompanied with the decreased frequency of high-affinity type mutation of W33L at the V_H186.2 in NP-binding IgG1$^+$ B cells (5). Several possibilities might be considered to explain the mechanism of GANP in generation of high-affinity BCR$^+$ B cells in vivo. GANP might be directly linked in genetic alteration, including *V* region dsDNA breaks occurring in B cell proliferation (23), SHM events in association with activation-induced cytidine deaminase (24), uracil DNA glycosylase (25), and error-prone DNA polymerases up-regulated in GC B cells (26), DNA recombination and repair mechanisms or rather involved in the selection of high-affinity BCR$^+$ B cells in the follicular dendritic cell network (27), and survival and maintenance of B cells with high-affinity type mutations throughout the immune response.

There are several possible mechanisms regarding the GANP function. Firstly, GANP might directly regulate generation of mutation frequency of the V_H region in GC B cells. The structure and expression of GANP indicated that GANP has two nuclear localization signal sequences (^{497}HKKK and ^{1344}PMKQKRR), two putative nuclear export signal sequences, and appears mostly in the nucleus but is also in the cytoplasm (our unpublished observation). The C-terminal region is capable of binding and acetylating with MCM3 of the MCM-complex that bears DNA helicase activity and is essential for DNA replication (28). In the N-terminal side, there is a putative RNA-associated region as the RNA recognition motif. The RNA-primase region and the RNA-binding activity might cooperate during the transcription at G_1 phase and introduce the alteration or the damage of the V_H region sequences during rapid cell proliferation in GCs. More interestingly, altered expression of

mouse SHD1 that has a homology to the central part of GANP (630–950 aa) caused an apparent cell cycle abnormality involving with centrosome duplication and M phase transition (29), which was also in accordance with the information of the association of *Saccharomyces* Sac3 with Cdc31/centrin (30). Loss of SHD1 caused an impairment of centrosome duplication, deregulated nuclear division, with disappearance of Mad2 expression in the prometaphase. Because mouse GANP is considered as a homologue of *Saccharomyces* Sac3 (31), GANP might be also involved in the centrosome duplication or the chromatin segregation during cell division. These observations suggested the involvement of GANP in either one or several mechanisms of gene transcription, DNA replication, and chromatin separation and cell division. Loss of GANP caused the increased apoptotic cells in GCs after immunization with TD-Ags (4), whereas the gain of function did not show obvious difference (data not shown). Second, these functions of GANP regions might be involved in the repair of DNA injuries occurring under a transcription-coupled mechanism or in the DNA replication phase. If this is the case, existence of GANP is critical for maintenance of DNA stability during the GC B cell stage that undergoes genetic alteration with frequent SHM of the V_H region and class switch recombination. Expression of GANP is necessary for the rescue of damaged GC B cells that potentially gain the high-affinity BCR. Third, additional function of GANP might be involved in generation or selection of high-affinity BCR^+ B cells in GCs. $Ganp^{Tg}$ mice showed accelerated kinetics of GC formation (Fig. 1*F*), whereas B-$ganp^{-/-}$ mice showed retarded GC formation (4). Recently, Mirnics et al. (32) described that GANP is involved in downstream event(s) of Lyn. As Lyn is involved in CD40-mediated signal transduction (33) and Lyn-deficient mice showed lack of GCs (34), there might be functional interaction of CD40-mediated signaling with the GANP function involved in regulation of high-affinity B cells. The augmented anti-CD40 response of $Ganp^{Tg}$ mice might support this notion, in which GANP is necessary for the rescue of high-affinity B cells during the selection in GCs. As a potential role of GANP in the selection process, GANP associates with a protein phosphatase component G5PR that associates with protein phosphatase 5 and protein phosphatase 2A (35). The complex of GANP with G5PR may regulate the other signaling pathways involved in cell survival mechanism or in regulation of BCR-mediated cell proliferation during maturation and selection of GC B cells. We have no definitive evidence to conclude the molecular mechanism at present but GANP is most likely a key molecule to elucidate the molecular mechanism in generation of high-affinity Ab in vivo.

To confirm the effect of GANP in generation of high-affinity Ab, we used a system to compare the affinity of the Abs at the monoclonal level by establishing the mAb-producing hybridomas. Affinity measurement with NP-hapten clearly demonstrated the high affinity of the mAbs generated from the $Ganp^{Tg}$ mice. Sequence analyses of the *V* regions of individual mAb-producing hybridomas demonstrated that the high affinity was generated not only with increased SHM frequency in the $V_H186.2$ region but also with the noncanonical V_H region usage that was not seen in the control hybridomas.

The results of both the loss and gain of GANP expression caused adverse effects in generation of high affinity response, which confirmed that the GANP function is involved in generation of high-affinity Ab in vivo. Additionally, the high-affinity is generated with the genetic alteration of *V* region genes as increased SHM and the different *V* region usage. GANP function might be directly involved in the formation of high affinity V region of the GC B cells. GANP is not up-regulated in the nonimmunized condition and is not expressed in normal T cells at the similar level detected with anti-GANP mAb (3). We speculate that up-regulation of GANP is selective in the cells with frequent genetic alterations such as *V* region SHM and class switch recombination during rapid proliferation phase.

In summary, we have demonstrated that $Ganp^{Tg}$ induces higher affinity Ab against TD-Ag in vivo, which was confirmed by BIAcore system with the purified mAbs against two model Ags of NP-hapten and the gp120 V3 peptide of HIV-1 by immunizing as TD-Ag. More importantly, the usage and the mutations of the V regions demonstrated that increased expression of GANP caused the genetic alteration of the *V* regions with increased mutations generating high affinity against TD-Ag in vivo. The results suggest that the $Ganp^{Tg}$ mouse has an advantage in preparation of mAbs against various epitopes, for which conventional mice hardly generate high-affinity mAbs by the standard procedures. High-affinity mAbs generated this way show greater epitope binding constants and this binding is long-lasting as measured in vitro. It would be useful to generate high-affinity mAbs against various molecules, which can be applicable widely in the diagnostic and therapeutic purposes.

Acknowledgments

We appreciate Dr. Y. Takahashi and Dr. T. Takemori for helpful advice and Y. Kumamoto for technical assistance.

Disclosures

The authors have no financial conflict of interest.

References

1. MacLennan, I. C. M. 1994. Germinal centers. *Annu. Rev. Immunol. 12:117.*
2. Rajewsky, K. 1996. Clonal selection and learning in the antibody system. *Nature 381:751.*
3. Kuwahara, K., M. Yoshida, E. Kondo, A. Sakata, Y. Watanabe, E. Abe, Y. Kouno, S. Tomiyasu, S. Fujimura, T. Tokuhisa, et al. 2000. A novel nuclear phosphoprotein, GANP, is up-regulated in centrocytes of the germinal center and associated with MCM3, a protein essential for DNA replication. *Blood 95:2321.*
4. Kuwahara, K., S. Tomiyasu, S. Fujimura, K. Nomura, Y. Xing, N. Nishiyama, M. Ogawa, S. Imajoh-Ohmi, S. Izuta, and N. Sakaguchi. 2001. Germinal center-associated nuclear protein (GANP) has a phosphorylation-dependent DNA-primase activity that is up-regulated in germinal center regions. *Proc. Natl. Acad. Sci. USA 98:10279.*
5. Kuwahara, K., S. Fujimura, Y. Takahashi, N. Nakagata, T. Takemori, S. Aizawa, and N. Sakaguchi. 2004. Germinal center-associated nuclear protein contributes to affinity maturation of B cell antigen receptor in T cell-dependent responses. *Proc. Natl. Acad. Sci. USA 101:1010.*
6. Koike, M., Y. Kikuchi, A. Tominaga, S. Takaki, K. Akagi, J. Miyazaki, K. Yamamura, and K. Takatsu. 1995. Defective IL-5-receptor-mediated signaling in B cells of X-linked immunodeficient mice. *Int. Immunol. 7:21.*
7. Jonsson, U., L. Fagerstam, B. Ivarsson, B. Johnsson, R. Karlsson, K. Lundh, S. Lofas, B. Persson, H. Roos, I. Ronnberg, et al. 1991. Real-time biospecific interaction analysis using surface plasmon resonance and a sensor chip technology. *BioTechniques 11:620.*
8. Johnsson, B., S. Lofas, and G. Lindquist. 1991. Immobilization of proteins to a carboxymethyldextran-modified gold surface for biospecific interaction analysis in surface plasmon resonance sensors. *Anal. Biochem. 198:268.*
9. Karlsson, R., A. Michaelsson, and L. Mattsson. 1991. Kinetic analysis of monoclonal antibody-antigen interactions with a new biosensor based analytical system. *J. Immunol. Methods 145:229.*
10. Furukawa, K., A. Akasako-Furukawa, H. Shirai, H. Nakamura, and T. Azuma. 1999. Junctional amino acids determine the maturation pathway of an antibody. *Immunity 11:329.*
11. Chen, J., P. Borden, J. Liao, and E. A. Kabat. 1992. Variable region cDNA sequences of three mouse monoclonal anti-idiotypic antibodies specific for anti-$\alpha_{1\text{—}6}$ dextrans with groove- or cavity-type combining sites. *Mol. Immunol. 29:1121.*
12. Wei, C., R. Zeff, and I. Goldschneider. 2000. Murine pro-B cells require IL-7 and its receptor complex to up-regulate IL-7Rα, terminal deoxynucleotidyltransferase, and cμ expression. *J. Immunol. 164:1961.*
13. Kimura, T., K. Yoshimura, K. Nishihara, Y. Maeda, S. Matsumi, A. Koito, and S. Matsushita. 2002. Reconstitution of spontaneous neutralizing antibody response against autologous human immunodeficiency virus during highly active antiretroviral therapy. *J. Infect. Dis. 185:53.*
14. Reed, L. J., and H. Muench. 1938. A simple method of estimating fifty percent end points. *Am. J. Hyg. 27:493.*
15. Jacob, J., G. Kelsoe, K. Rajewsky, and U. Weiss. 1991. Intraclonal generation of antibody mutants in germinal centres. *Nature 354:389.*
16. Jacob, J., J. Przylepa, C. Miller, and G. Kelsoe. 1993. In situ studies of the primary immune response to (4-hydroxy-3-nitrophenyl)acetyl. III. The kinetics of

V region mutation and selection in germinal center B cells. *J. Exp. Med. 178:1293.*
17. Cumano, A., and K. Rajewsky. 1986. Clonal recruitment and somatic mutation in the generation of immunological memory to the hapten NP. *EMBO J. 5:2459.*
18. Allen, D., T. Simon, F. Sablitzky, K. Rajewsky, and A. Cumano. 1988. Antibody engineering for the analysis of affinity maturation of an anti-hapten response. *EMBO J. 7:1995.*
19. French, D. L., R. Laskov, and M. D. Scharff. 1998. The role of somatic hypermutation in the generation of antibody diversity. *Science 244:1152.*
20. Poignard, P., T. Fouts, D. Naniche, J. P. Moore, and Q. J. Sattentau. 1996. Neutralizing antibodies to human immunodeficiency virus type-1 gp120 induce envelope glycoprotein subunit dissociation. *J. Exp. Med. 183:473.*
21. Kimpton, J., and M. Emerman. 1992. Detection of replication-competent and pseudotyped human immunodeficiency virus with a sensitive cell line on the basis of activation of an integrated β-galactosidase gene. *J. Virol. 66:2232.*
22. Matsushita, S., H. Maeda, K. Kimachi, Y. Eda, Y. Maeda, T. Murakami, S. Tokiyoshi, and K. Takatsuki. 1992. Characterization of a mouse/human chimeric monoclonal antibody (Cβ1) to a principal neutralizing domain of the human immunodeficiency virus type 1 envelope protein. *AIDS Res. Hum. Retroviruses 8:1107.*
23. Wu, X., J. Feng, A. Komori, E. C. Kim, H. Zan, and P. Casali. 2003. Immunoglobulin somatic hypermutation: double-strand DNA breaks, AID and error-prone DNA repair. *J. Clin. Immunol. 23:235.*
24. Honjo, T., K. Kinoshita, and M. Muramatsu. 2002. Molecular mechanism of class switch recombination: linkage with somatic hypermutation. *Annu. Rev. Immunol. 20:165.*
25. Storb, U., and J. Stavnezer. 2002. Immunoglobulin genes: generating diversity with AID and UNG. *Curr. Biol. 12:R725.*
26. Jacobs, H., and L. Bross. 2001. Towards an understanding of somatic hypermutation. *Curr. Opin. Immunol. 13:208.*
27. van Eijk, M., T. Defrance, A. Hennino, and C. de Groot. 2001. Death-receptor contribution to the germinal-center reaction. *Trends Immunol. 22:677.*
28. Bailis, J. M., and S. L. Forsburg. 2004. MCM proteins: DNA damage, mutagenesis and repair. *Curr. Opin. Genet. Dev. 14:17.*
29. Khuda, S. E., M. Yoshida, Y. Xing, T. Shimasaki, M. Takeya, K. Kuwahara, and N. Sakaguchi. 2004. The *Sac3* homologue *shd1* is involved in mitotic progression in mammalian cells. *J. Biol. Chem. 279:46182.*
30. Fischer, T., S. Rodriguez-Navarro, G. Pereira, A. Racz, E. Schiebel, and E. Hurt. 2004. Yeast centrin Cdc31 is linked to the nuclear mRNA export machinery. *Nat. Cell Biol. 6:840.*
31. Bauer, A., and R. Kölling. 1996. Characterization of the SAC3 gene of *Saccharomyces cerevisiae. Yeast 12:965.*
32. Mirnics, Z. K., E. Caudell, Y. Gao, K. Kuwahara, N. Sakaguchi, T. Kurosaki, J. Burnside, K. Mirnics, and S. J. Corey. 2004. Microarray analysis of Lyn-deficient B cells reveals germinal center-associated nuclear protein and other genes associated with the lymphoid germinal center. *J. Immunol. 172:4133.*
33. Ren, C. L., T. Morio, S. M. Fu, and R. S. Geha. 1994. Signal transduction via CD40 involves activation of *lyn* kinase and phosphatidylinositol-3-kinase, and phosphorylation of phospholipase Cγ2. *J. Exp. Med. 179:673.*
34. Nishizumi, H., I. Taniuchi, Y. Yamanashi, D. Kitamura, D. Ilic, S. Mori, T. Watanabe, and T. Yamamoto. 1995. Impaired proliferation of peripheral B cells and indication of autoimmune disease in *lyn*-deficient mice. *Immunity 3:549.*
35. Kono, Y., K. Maeda, K. Kuwahara, H. Yamamoto, E. Miyamoto, K. Yonezawa, K. Takagi, and N. Sakaguchi. 2002. MCM3-binding GANP DNA-primase is associated with a novel phosphatase component G5PR. *Genes Cells 7:821.*

分担研究者　森内　浩幸

発表者氏名	論文タイトル名	発表誌名	巻号	ページ	出版年
Moriuchi M, Yoshimine H, Oishi K, and **Moriuchi H**.	Norepinephrine inhibits human immunodeficiency virus type-1 infection through the NF-kappaB inactivation.	***Virology***	345	167-173	2006

Available online at www.sciencedirect.com
SCIENCE DIRECT
ELSEVIER
Virology 345 (2006) 167 – 173
VIROLOGY
www.elsevier.com/locate/yviro

Norepinephrine inhibits human immunodeficiency virus type-1 infection through the NF-κB inactivation

Masako Moriuchi [a], Hiroyuki Yoshimine [c], Kazunori Oishi [c], Hiroyuki Moriuchi [a,b,*]

[a] *Division of Medical Virology, Department of Molecular Microbiology and Immunology, Nagasaki University Graduate School of Biomedical Sciences, Nagasaki 852-8523, Japan*
[b] *Department of Pediatrics, Nagasaki University Hospital, Nagasaki 852-8501, Japan*
[c] *Department of Internal Medicine, Institute of Tropical Medicine, Nagasaki University, Nagasaki 852-8523, Japan*

Received 5 July 2005; returned to author for revision 26 August 2005; accepted 4 October 2005
Available online 4 November 2005

Abstract

Exercise or acute stress can exert significant effects on immune system as well as cardiovascular and respiratory systems through catecholamines. In this study, we investigated effects of norepinephrine (NE), a catecholamine neurotransmitter on human immunodeficiency virus type-1 (HIV-1) infection. NE inhibited in vitro HIV-1 infection of peripheral blood mononuclear cells (PBMC) from healthy donors and ex vivo HIV-1 replication in patients' PBMC. In transient expression assays, NE downregulated HIV-1 long terminal repeat, but site-directed mutagenesis on NF-κB-binding sites or cotreatment with H89 (a protein kinase A inhibitor) abrogated the NE-mediated effect. Gel-shift assays showed suppression of NF-κB activity in NE-treated cells. NE increased cytoplasmic levels of IκB-α, a natural inhibitor of NF-κB. Thus, NE apparently inhibits HIV-1 infection, at least in part through NF-κB inactivation.

Keywords: HIV-1; Norepinephrine; Catecholamines; Stress; NF-κB; Long terminal repeat

Introduction

A number of host, viral and environmental factors have been shown to influence the pathogenesis of human immunodeficiency virus type-1 (HIV-1) disease. Events in daily lives may thus have some impacts on HIV-1 infection through interactions between those factors. Exercise as well as acute psychological stress leads to activation of the sympathetic nervous system (SNS), which is mediated by neurotransmitters such as norepinephrine (NE). NE exerts not only cardiotonic and bronchodilating actions but also anti-inflammatory effects.

A number of previous studies have demonstrated that β-adrenergic agonists suppress production of proinflammatory cytokines such as tumor necrosis factor-α, interleukin (IL)-1β and IL-6 (Cole et al., 1998; Farmer and Pugin, 2000; Heneka et al., 2003; Koff et al., 1986; Severn et al., 1992; Talmadge et al., 1993; Van der Poll et al., 1994). Since the pathogenesis of HIV-1 infection is deeply involved in immune activation, NE may influence HIV-1 infection as well as cytokine networks. In this study, we show that NE inhibited HIV-1 infection, at least in part, by downregulation of NF-κB activity.

Results and discussion

NE suppresses HIV-1 replication

NE effects on HIV-1 infection were investigated in two systems. In in vitro or acute infection system, peripheral blood mononuclear cells (PBMC) and monocyte-derived macrophages (MDM) were isolated from healthy individuals, and were infected in vitro with R5 (AD8)- or X4 (NL4-3)-HIV-1. PBMC that had been prestimulated with anti-CD3 and anti-CD28 antibodies were treated with NE prior to infection and throughout the incubation period. The concentrations of NE used in these experiments were between 10 nM and 1 μM, since serum NE levels reach 10 nM upon activation of the SNS (Bierhaus et al., 2003) and NE is released neuronally into the

* Corresponding author. Department of Pediatrics, Nagasaki University Hospital, Nagasaki 852-8501, Japan.
E-mail address: hiromori@net.nagasaki-u.ac.jp (H. Moriuchi).

0042-6822/$ - see front matter © 2005 Elsevier Inc. All rights reserved.
doi:10.1016/j.virol.2005.10.002

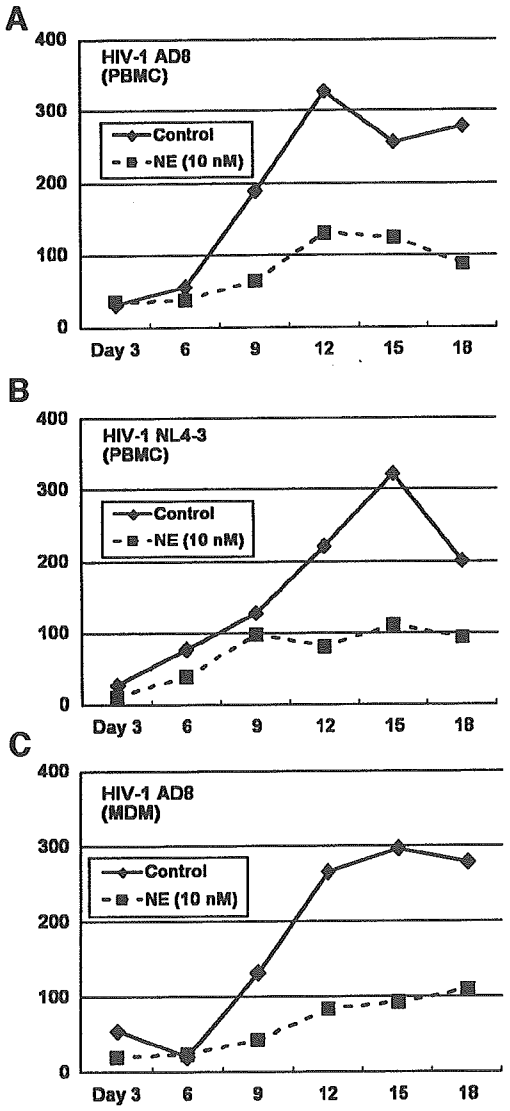

Fig. 1. NE inhibited HIV-1 infection of PBMC or MDM. (A, B) PBMC from a healthy donor were prestimulated with anti-CD3 and anti-CD28 antibodies for 2 days and infected with HIV-1 AD8 (A) or HIV-1 NL4-3 (B). One set of culture was also treated with NE (10 nM) 24 h prior to and after infection and RT assays were performed for cell-free culture supernatants. Similar results were obtained from 3 different donors (data not shown). (C) MDM from a healthy donor were either untreated or treated with NE (10 nM) 24 h prior to and after infection with HIV-1 AD8, and RT assays were performed for cell-free culture supernatants. Similar results were obtained from 3 different donors (data now shown).

lymphoid tissue at micromolar levels (Felten et al., 1987). As shown in Fig. 1, HIV-1 replication was reduced in the presence of 10 nM of NE, irrelevantly to HIV-1 phenotypes (R5 versus X4) or target cells (PBMC versus MDM). Higher concentrations of NE (100 nM or 1 μM) had slightly more potent anti-HIV-1 effects, but prolonged (>1 week) exposure to NE higher than 10 nM was variably toxic to PBMC in trypan blue exclusion assays and 3-(4,5-dimethylthiazol-2-yl)-2,5-dimethyltetrazolium bromide (MTT) assays (data not shown); therefore, higher concentrations were not applied to infection experiments thereafter. In contrast, percentages (mean ± SD) of viable cells in the presence of NE (10 nM) were comparable to those in the absence of NE (86% ± 8% versus 89% ± 9%).

NE effects were also investigated in PBMC derived from HIV-1-infected individuals, some of which had been on highly active antiretroviral therapy (HAART) (Table 1). Ex vivo stimulation of $CD8^+$ T cell-depleted PBMC with anti-CD3 and anti-CD28 induced endogenous HIV-1 replication; however, cotreatment with NE precluded such HIV-1 outgrowth (Table 1). Thus, NE appears to suppress HIV-1 infection in both in vitro (acute) and ex vivo (endogenous) experimental conditions.

To demonstrate whether NE-mediated effect is specific to HIV-1, we also tested NE effects on infection with human T-cell leukemia virus type I (HTLV-I), another human retrovirus. PBMC derived from asymptomatic HTLV-I carriers were incubated in the presence or absence of NE (10 nM), and release of HTLV-I virions into culture medium as well as proviral load in cells was determined. NE did not suppress ex vivo HTLV-I infection, and contrarily, did enhance it slightly (Table 2). Therefore, NE-mediated anti-HIV-1 activity does not appear to be a non-specific effect.

To investigate at which step(s) in the HIV replication cycle NE exerts its influence, we performed single-round viral replication assays using replication-incompetent luciferase-reporter molecular clone NL43-Luc-R^-E^- that had been complemented with R5-tropic (ADA), X4-tropic (HXB2) or amphotropic (murine leukemia virus [MLV]) Env glycoprotein. Either pretreatment or post-treatment with NE inhibited HIV-1 infection of anti-CD3/anti-CD28-stimulated PBMC or MDM in physiologically relevant concentrations in serum (10 nM) or the lymphoid tissue (1 μM), and NE had similar influence on R5-tropic, X4-tropic or amphotropic virus (Figs. 2A–B).

Table 1
NE suppressed HIV-1 outgrowth by cellular activation

Patient no. (age/gender)	Antiviral therapy	Viral RNA (copies/ml)	CD4 T cell counts (cells/mm^3)	RT activity (cpm/μl)		
				No stimulation	Anti-CD3/CD28	Anti-CD3/CD28 + NE
1 (57 M)	ZDV/3TC/NFV	<50	802	<40	224	<40
2 (54 F)	ZDV/ddC/NFV	<50	432	<40	333	<40
3 (34 M)	No therapy	6900	592	<40	1264	168
4 (25 M)	No therapy	4400	451	<40	658	<40

ZDV, zidovudine; 3TC, lamivudine; ddC, zalcitabine; NFV, nelfinavir.
Approximately one million CD8-depleted PBMC derived from the above patients were incubated in the presence or absence of anti-CD3 and anti-CD28 antibody ± NE (10 nM). Maximal RT activities obtained from cell-free supernatants during 21-day culture period are shown.

Table 2
NE slightly enhanced HTLV-I replication

Patient no.	Proviral load (copies/100 PBMC)		p19 (pg/ml)	
	No stimulation	NE (10 nM)	No stimulation	NE (10 nM)
1	0.24	0.30	65	80
2	0.12	0.29	<25	62
3	0.082	0.19	<25	<25
4	0.82	0.91	286	342

Approximately one million PBMC were incubated in the presence or absence of NE (10 nM). Cell-free culture supernatants were collected for p19 assays, and DNA was extracted from cell pellets for real-time PCR of HTLV-I provirus.

To further investigate at which step(s) in the HIV replication cycle NE exerts its influence, we quantified HIV-1 proviral DNA loads 24 h after infection by real-time PCR. Pretreatment of PBMC or MDM with NE had little effect on HIV-1 proviral DNA loads in those experiments (Fig. 2C), indicating that NE could not inhibit HIV-1 entry into cells. Furthermore, NE treatment had little effects on cell surface expression of CD4, CCR5 or CXCR4 (data not shown). Those results suggested that post-entry step(s) are involved mostly in NE-mediated suppression of HIV-1 infection.

NE downregulates HIV-1 long terminal repeat (LTR) promoter

To investigate mechanisms whereby NE inhibits HIV-1 infection, we tested NE effects on HIV-1 transcription, one of the most critical post-entry steps of viral replicative cycle.

NE downregulated HIV-1 LTR activity in either cell type (Figs. 3A–B; data not shown), and deletion of NF-κB-binding sites, but not of SP1-binding sites abrogated the NE-mediated effect (Figs. 3A–B).

NE-mediated downregulation of HIV-1 LTR involves inhibition of NF-κB activity

Since the aforementioned results suggested that NF-κB-binding sites were required for NE-mediated downregulation of HIV-1 LTR activity, NF-κB activity was determined by gel-mobility shift assay in nuclear extracts from NE-treated or untreated THP-1 cells. THP-1 cells had constitutional NF-κB activity (formation of p50/p65 heterodimer) (Fig. 3C), which was enhanced by stimulation with phorbol 12-myristate 13-acetate (PMA) (Fig. 3D); however, NE treatment markedly suppressed p50/p65 heterodimer formation in a dose-dependent manner (Figs. 3D–E). In contrast, NE had no or little effect on SP1 activity (Fig. 3D).

Inhibition of NF-κB activity could result either from competition of NF-κB-binding sites on HIV-1 LTR with other transcription factor(s) or from the regulation by its natural inhibitor, IκB-α. If the former postulation was the case, gel-mobility shift assays should have shown formation of a novel complex on the NF-κB element. However, since we only observed diminishment of NF-κB complex, not formation of a novel complex, downregulation of NF-κB activity by IκB-α is more likely. To verify this postulation, two experiments were done. First, transient expression assays were performed in the presence of NE ± H89, a protein kinase A (PK-A) inhibitor. It has been shown that signaling of NE or other β-agonists via β-adrenergic receptor is mediated by PK-A, and that PK-A inhibitors prevent such activity. As expected, NE-mediated downregulation of HIV-1 LTR was significantly neutralized by H89 (Fig. 3F). Second, Western blot analysis was performed to determine cytoplasmic IκB-α levels inTHP-1 cells that had been untreated or treated with NE ± H89. As shown in Fig. 3G, NE treatment increased cytoplasmic IκB-α levels, but H89 counteracted NE. Those results suggested that NE down-

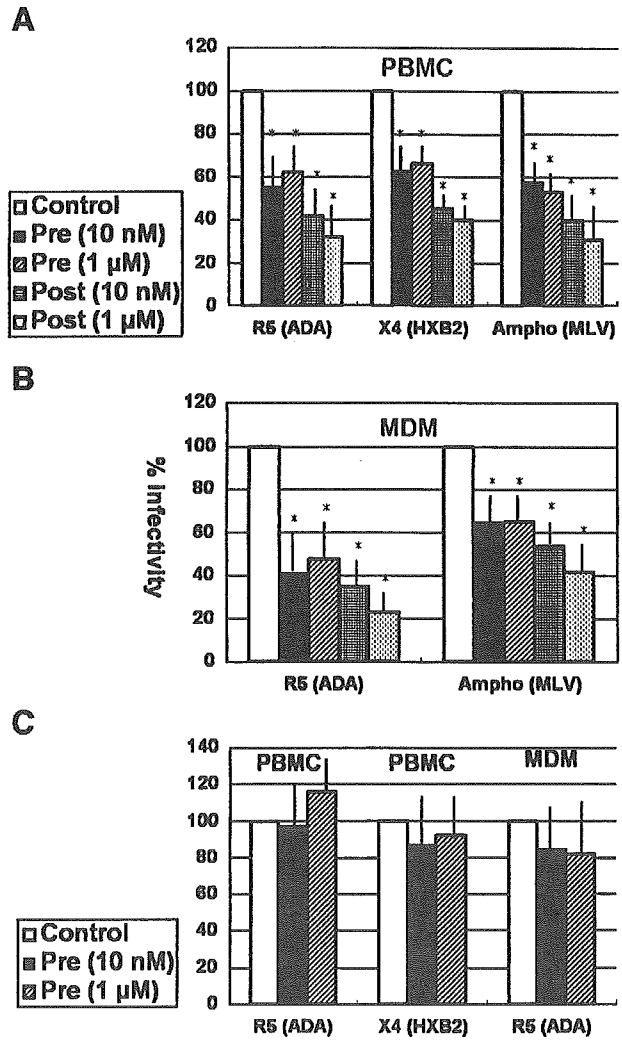

Fig. 2. NE inhibited HIV-1 infection at post-entry step(s). (A, B) Either pretreatment or post-treatment with NE inhibited HIV-1 infection. PBMC prestimulated with anti-CD3 and anti-CD28 (A) or MDM (B) from healthy donors were incubated with HIV-1 NL4-3-Luc-R$^-$E$^-$ complemented with the indicated Env glycoprotein. Where indicated, the cells were treated with 10 nM or 1 μM of NE for 24 h prior to infection (Pre) or immediately after infection (Post). The data shown are representative of three independent experiments from separate donors yielding similar results, as the mean (±SD) of triplicate determinations. Statistically significant differences between control and NE treatment are indicated by $^*P < 0.05$. (C) NE had little effect on HIV-1 entry into cells. PBMC prestimulated with anti-CD3 and anti-CD28 or MDM from healthy donors were infected with the indicated viruses, and HIV-1 proviral loads were quantified by real-time PCR 24 h after infection. The data shown are representative of three independent experiments from separate donors yielding similar results, as the mean (±SD) of triplicate determinations. Statistically significant differences between control and NE were not obtained.

regulated HIV-1 LTR, at least in part, through inhibition of NF-κB activity.

In this study, we have shown that NE inhibited HIV-1 replication in both acute and endogenous infection systems, and in both PBMC and MDM. Our results also suggested that downregulation of NF-κB activity was involved in NE-mediated anti-HIV-1 effect.

NE effects on NF-κB activity have been controversial in the previous reports. While several studies demonstrated that NE increases expression of I-κBα, which inhibits NF-κB activity (Farmer and Pugin, 2000; Gavrilyuk et al., 2002; Heneka et al., 2003), a recent study has shown that NE induces NF-κB activity (Bierhaus et al., 2003). The reason why NE and/or other catecholamines apparently mediated quite different effects on NF-κB activity is unknown. The inhibitory effect was demonstrated in THP-1 cells (Farmer et al., 2000; this study), PBMC (this study), astrocytes (Gavrilyuk et al., 2002) or brain tissue (Heneka et al., 2003); induction of NF-κB activity was shown in PBMC and THP-1 cells (Bierhaus et al., 2003). Therefore, such discrepancy cannot be explained by difference in cell types tested. Although our study suggested that PK-A-mediated NE signaling increased I-κBα levels, more precise molecular mechanisms remain obscure. Further studies are needed to clarify the apparent controversy and to define more detailed cellular and molecular mechanisms. We are currently investigating them.

It may be difficult to precisely determine net effects of exercise or acute stress on HIV-1 infection, since a number of factors are involved in those conditions. Although we have demonstrated that NE, one of the mediators involved in exercise or acute stress, inhibited HIV-1 infection, we do not believe that adequate burden of stress simply leads to modulation of HIV-1 replication in infected individuals. However, it may be worthwhile investigating potential benefit of exercise in HIV-1-infected individuals, since exercise induces the SNS activity but probably not other detrimental effects observed in stress reactions (Cole and Kemeny, 1997). In this regard, it has been reported that NE response to stress is blunted in HIV-1-infected individuals (Kumar et al., 1991), and that a cerebrospinal fluid catecholamine metabolite is lower in AIDS patients (Lasson et al., 1991). In addition, Cole et al. (2001) have recently shown that high autonomic nervous activity is associated with impaired response to HAART in HIV-infected individuals. Thus, it might be possible that individuals with high autonomic nervous system activity may be somehow different from those with low activity in their immunological activity or drug metabolism, and that HIV-1 infection itself may lead to autonomic dysfunction. Further investigations are needed to clarify these issues.

Materials and methods

In vitro or acute HIV-1 infection experiments

PBMC were isolated from healthy individuals, and propagated as described previously (Moriuchi et al., 1998b). Monocytes were isolated from PBMC by sorting $CD14^+$ cells with AutoMACS (Moriuchi and Moriuchi, 2004b), and monocyte-derived macrophages (MDM) were propagated as described previously (Moriuchi et al., 1998b). R5 (AD8)- and X4 (NL4-3)-HIV-1 stocks were propagated by transfecting 293T cells with the corresponding plasmids (Moriuchi et al., 1998b). PBMC that had been prestimulated with anti-CD3 and anti-CD28 antibodies (1 μg/ml each) for 2 days, or 7-day-old MDM, were treated with NE (Sigma Chemical Co., St. Louis, MO) 24 h prior to infection and throughout the incubation period. Cell-free culture supernatants were collected every 3 days for reverse transcriptase (RT) assays (Moriuchi et al., 1998a).

Ex vivo or endogenous HIV-1 infection experiments

PBMC were isolated from HIV-1-infected patients outlined in Table 1, and $CD8^+$ T cells were depleted as described previously (Moriuchi et al., 1998a). Approximately one million CD8-depleted PBMC were incubated in RPMI-1640 with 10% fetal bovine serum in the presence or absence of anti-CD3 and anti-CD28 antibody (1 μg/ml each) ± NE (10 nM). Cell-free supernatants were collected every 3 days until day 21, and tested for RT activity.

Ex vivo or endogenous HTLV-I infection experiments

PBMC were isolated from asymptomatic HTLV-I carriers, and approximately one million PBMC were incubated in RPMI-1640 with 10% fetal bovine serum in the presence or absence of

Fig. 3. NE downregulated HIV-1 LTR activity through inhibition of NF-κB activity. (A, B) NE downregulated HIV-1 LTR, and NF-κB-binding sites are apparently involved in the NE-mediated effect. PBMC (A) or MDM (B) were transfected with the indicated reporter plasmid along with pSV2-Tat, either untreated or treated with NE (10 nM) for 24 h, and harvested for luciferase assays 2 days after transfection. Arbitrary light units of promoter-less pGL2-basic transfectants were always less than 3 (data not show). The data shown are representative of three independent experiments from separate donors yielding similar results, as the mean (±SD) of triplicate determinations. Statistically significant differences between control and NE treatment are indicated by $*P < 0.05$. (C) Constitutive NF-κB activity in THP-1 cells. Nuclear extracts were prepared from THP-1 cells, and gel-mobility shift assays were performed using an oligonucleotides corresponding to HIV-1 LTR NF-κB-binding sites as a probe (Moriuchi and Moriuchi, 2004a, 2004b). Where indicated, control serum or antibodies to p50 or p65 were added to the reaction. Identification of protein–DNA complexes was indicated. (D, E) Inhibition of NF-κB, but not SP1 in NE-treated THP-1 cells. THP-1 cells were either untreated or treated with NE (10 nM or 1 μM) or PMA before harvest for nuclear extract preparation. Gel shift assays were performed using probes corresponding to HIV-1 LTR NF-κB-binding sites or SP1-binding sites. Similar results were obtained in nuclear extracts of PBMC derived from 3 different donors (data not shown). (F, G) NE-mediated inhibition of NF-κB activity involves PK-A pathway. (F) Transient expression assays. THP-1 cells were transfected with pGL-HIV-1-LTR and pSV2-Tat, were untreated or treated with NE (1 μM) ± H89 (10 μM), and cell lysates were tested for luciferase activity. The data shown are representative of three independent experiments from separate donors yielding similar results, as the mean (±SD) of triplicate determinations. Statistically significant differences between control and NE treatment are indicated by $*P < 0.05$. (G) Western blot analysis. Cell lysates from untreated THP-1 cells (lane 1), THP-1 cells treated with NE (1 μM) alone (lane 2) or THP-1 cells treated with both NE and H89 (10 μM) (lane 3) were analyzed by Western blotting for cytoplasmic IκB-α levels. The same set of cell lysates were also analyzed for actin (lanes 4–6).

NE (10 nM) for 7 days. Assays of p19 antigen levels in cell-free supernatants and of proviral DNA in PBMC were performed as described previously (Moriuchi and Moriuchi, 2004a).

Single-round viral replication assays

Replication-incompetent luciferase-reporter molecular clone NL43-Luc-R$^-$E$^-$ was complemented with R5-tropic (ADA), X4-tropic (HXB2) or amphotropic (murine leukemia virus [MLV]) Env glycoprotein by cotransfecting 293T cells with plasmids encoding the corresponding Env glycoproteins (Moriuchi et al., 1998b). Anti-CD3/anti-CD28-prestimulated PBMC or MDM were either untreated or treated with NE (10 nM) for 24 h, infected with those virus stocks for 3 h, and infectivity was estimated by luciferase assays that were performed 48 h after infection (Moriuchi et al., 1998a).

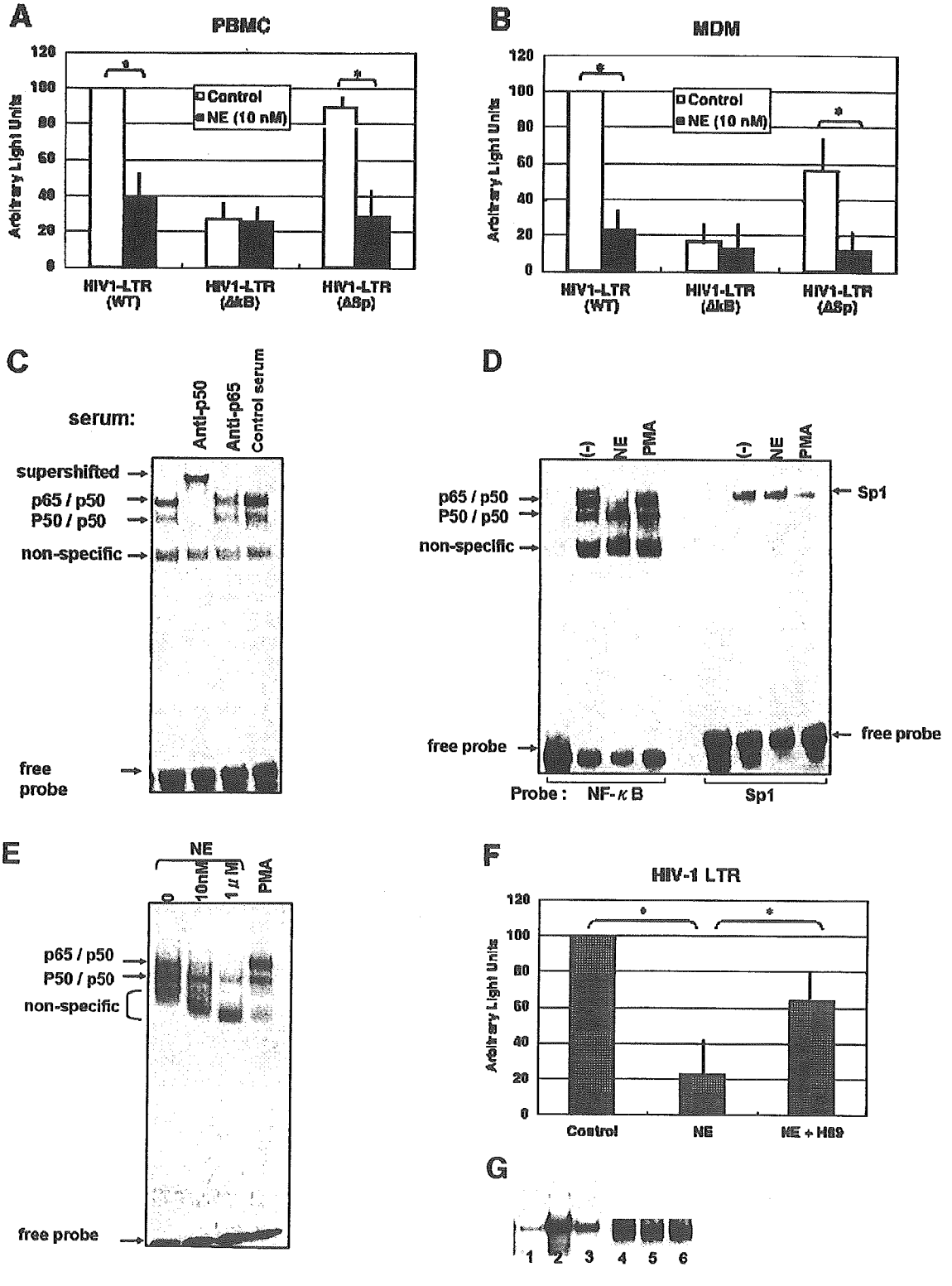

HIV-1 entry assays

PBMC that had been prestimulated with anti-CD3 and anti-CD28 antibodies or MDM were untreated or pretreated with NE (1 μM) for 24 h before infection with the indicated viruses. The infected cells were extensively washed 4 h after, and harvested 24 h after infection, RNA-free DNA was extracted, according to manufacturer's instruction (QIAamp DNA Mini Kits, QIAGEN K.K., Tokyo, Japan) and real-time quantitative PCR for HIV-1 proviral DNA of *gag* region was performed as described previously (Hoshino et al., 2004).

Cytotoxicity tests

Viability of cultured cells was assessed with trypan blue exclusion assays or 3-(4,5-dimethylthiazol-2-yl)-2,5-dimethyltetrazolium bromide (MTT) assays after NE treatment, according to the manufacturer's instructions (the CellTiter-Blue Cell Viability Assay, Promega K.K., Tokyo, Japan).

Plasmids and transfection

Plasmid pGL-HIV-1-LTR contains HIV-1 long terminal repeat (LTR) from HXB2 strain in pGL2-basic (Promega, Madison, WI) backbone. NF-κB and SP1 binding sites on HIV-1 LTR were deleted in plasmids pGL-HIV-1-LTRΔNF-κB and pGL-HIV-1-LTRΔSP1, respectively (Margolis et al., 1992). Transfection of PBMC and THP-1 cells was performed by electroporation (Moriuchi et al., 1997), and MDM were transfected by modified calcium phosphate method (Moriuchi et al., 1994).

Nuclear extracts, antibodies and gel-mobility shift assays

Nuclear extracts were prepared from THP-1 cells untreated or treated with NE for 60 min or PMA for 15 min (Sigma Chemical Co., St. Louis, MO), and gel-mobility shift assays were performed, as described previously (Moriuchi et al., 1997). Antibodies to p50 and p65 were kindly provided by U. Siebenlist (National Institutes of Allergy and Infectious Diseases, Bethesda, MD).

Western blotting

THP-1 cells were untreated or treated with NE ± H-89 (10 μM) (Sigma Chemical Co., St. Louis, MO) for 60 min, and lysed in RIPA buffer (10 mM Tris–HCl [pH 8.0], 100 mM NaCl, 1 mM EDTA, 1% NP-40, 0.5% deoxy cholate, 0.1% SDS and 100 μg/ml phenylmethylsulfonyl fluoride). Lysates from 5×10^5 cells were loaded in each lane, separated by SDS-PAGE (8% acrylamide-bis-acrylamide gel) and electrotransferred onto a nitrocellulose membrane (0.45 μm). IκB-α or actin was detected with rabbit anti-human IκB-α antibody (Santa-Cruz Biotechnology, Santa Cruz, CA) or rabbit anti-actin antibody (SIGMA-ALDRICH Japan, Tokyo, Japan), mouse anti-rabbit horseradish peroxidase-conjugated secondary antibody (Amersham Biosciences, Piscataway, NJ) and enhanced chemiluminescence reaction with ECL Plus Western Blotting Detection System (Amersham Biosciences).

Acknowledgments

We thank N. Landau, J. Sodroski, M. Martin, K. Peden and U. Siebenlist for reagents; Chiyoda, H. Okuda and K. Deguchi (Nagasaki Red Cross Blood Center) for blood samples; M. Yokoyama for excellent technical assistance; and Y. Matsuyama for graphic work. This work was supported in part by a grant provided by a Research for the Future Program (JSPS-RFTF97L00705) of the Japan Society for the Promotion of Science and by a Grant-in-Aid from the Ministry of Health, Labor and Welfare, Japan.

References

Bierhaus, A., Wolf, J., Andrassy, M., Rohleder, N., Humpert, P.M., Petrov, D., Ferstl, R., von Eynatten, M., Wendt, T., Rudofsky, G., Joswig, M., Morcos, M., Schwaninger, M., McEwen, B., Kirshbaum, C., Nawroth, P.P., 2003. A mechanism converting psychosocial stress into mononuclear cell activation. Proc. Natl. Acad. Sci. U.S.A. 100, 1920–1925.

Cole, S.W., Kemeny, M.E., 1997. Psychobiology of HIV infection. Crit. Rev. Neurobiol. 11, 289–321.

Cole, S.W., Korin, Y.D., Fahey, J.L., Zack, J.A., 1998. Norepinephrine accelerates HIV replication via protein kinase A-dependent effects on cytokine production. J. Immunol. 161, 610–616.

Cole, S.W., Naliboff, B.D., Kemeny, M.E., Griswold, M.P., Fahey, J.L., Zack, J.A., 2001. Impaired response to HAART in HIV-infected individuals with high autonomic nervous system activity. Proc. Natl. Acad. Sci. U.S.A. 98, 12695–12700.

Farmer, P., Pugin, J., 2000. β-Adrenergic agonists exert their "anti-inflammatory" effects in monocytic cells through the IκB/NF-κB pathway. Am. J. Physiol.: Lung Cell. Mol. Physiol. 279, L675–L682.

Felten, D.L., Felten, S.Y., Bellinger, D.L., Carlson, S.L., Ackerman, K.D., Madden, K.S., Olschowki, J.A., Livnat, S., 1987. Noradrenergic sympathetic neural interactions with the immune system: structure and function. Immunol. Rev. 100, 225–260.

Gavrilyuk, V., Russo, C.D., Heneka, M.T., Pelligrino, D., Weinberg, G., Feinstein, D.L., 2002. Norepinephrine increases I-κB expression in astrocytes. J. Biol. Chem. 277, 29662–29668.

Heneka, M.T., Gavrilyuk, V., Landreth, G.E., O'Banion, M.K., Weinberg, G., Feinstein, D.L., 2003. Noradrenergic depletion increases inflammatory responses in brain: effects on IκB and HSP70 expression. J. Neurochem. 85, 387–398.

Hoshino, Y., Tse, D.B., Rochford, G., Prabhakar, S., Hoshino, S., Chitkara, N., Kuwabara, K., Ching, E., Raju, B., Gold, J.A., Borkowsky, W., Rom, W.N., Pine, R., Weiden, M., 2004. Mycobacterium tuberculosis-induced CXCR4 and chemokine expression leads to preferential X4 HIV-1 replication in human macrophages. J. Immunol. 172, 6251–6258.

Koff, W.C., Fann, A.V., Dunegan, M.A., Lachman, L.B., 1986. Catecholamine-induced suppression of interleukin-1 production. Lymphokine Res. 5, 239–247.

Kumar, M., Morgan, R., Szapocznik, J., Eisdorfer, C., 1991. Norepinephrine response in early HIV infection. J. AIDS 4, 782–786.

Lasson, M., Hagberg, L., Forsman, A., Norkrans, G., 1991. Cerebrospinal fluid catecholamine metabolites in HIV-infected patients. J. Neurosci. Res. 28, 406–409.

Margolis, D.M., Rabson, A.B., Straus, S.E., Ostrove, J.M., 1992. Transactivation of the HIV-1 LTR by HSV-1 immediate-early genes. Virology 186, 788–791.

Moriuchi, M., Moriuchi, H., 2004a. Seminal fluid enhances replication of human T-cell leukemia virus type I: implications for sexual transmission. J. Virol. 78, 12709–12711.

Moriuchi, M., Moriuchi, H., 2004b. Cell-type-dependent effect of transforming

growth factor-β, a major cytokine in breast milk, on human immunodeficiency virus type 1 infection of mammary epithelial MCF-7 cells or macrophages. J. Virol. 78, 13046–13052.

Moriuchi, M., Moriuchi, H., Straus, S.E., Cohen, J.I., 1994. Varicella-zoster virus (VZV) virion-associated transactivator open reading frame 62 protein enhances the infectivity of VZV DNA. Virology 200, 297–300.

Moriuchi, H., Moriuchi, M., Fauci, A.S., 1997. NF-κB potently upregulates expression of RANTES, an anti-HIV chemokine. J. Immunol. 158, 3483–3491.

Moriuchi, H., Moriuchi, M., Fauci, A.S., 1998. Factors secreted by HTLV-I infected cells can enhance or inhibit replication of HIV-1 in HTLV-I uninfected cells: implication for in vivo coinfection with HTLV-I and HIV-1. J. Exp. Med. 187, 1689–1698.

Moriuchi, M., Moriuchi, H., Turner, W., Fauci, A.S., 1998. Exposure to bacterial products renders macrophages highly susceptible to T-tropic human immunodeficiency virus type 1: implications for in vivo coinfections. J. Clin. Invest. 102, 1540–1550.

Severn, A., Rapson, N.T., Hunter, C.A., Liew, F.Y., 1992. Regulation of tumor necrosis factor production by adrenaline and β-adrenergic agonists. J. Immunol. 148, 3441–3445.

Talmadge, J., Scott, R., Castelli, P., Newman-Tarr, T., Lee, J., 1993. Molecular pharmacology of the β-adrenergic receptor on THP-1 cells. Int. J. Immunopharmacol. 15, 219–228.

Van der Poll, T., Jansen, J., Endert, E., Sauerwein, H.P., van Deventer, S.J., 1994. Noradrenalin inhibits lipopolysaccharide-induced tumor necrosis factor and interleukin 6 production in human whole blood. Infect. Immun. 62, 2046–2050.

分担研究者　満屋　裕明

発表者氏名	論文タイトル名	発表誌名	巻号	ページ	出版年
Nakata H, Maeda K, Miyakawa T, Shibayama S, Matsuo M, Takaoka Y, Ito M, Koyanagi Y, and **Mitsuya H**.	Potent anti-R5 human immunodeficiency virus type 1 effects of a CCR5 antagonist, AK602/ONO4128/GW873140, in a novel human peripheral blood mononuclear cell nonobese diabetic-SCID, interleukin-2 receptor gamma-chain-knocked-out AIDS mouse model.	***J Virol***	79	2087-2096	2005
Ghosh AK, Swanson LM, Cho H, Leshchenko S, Hussain KA, Kay S, Walters DE, Koh Y, and **Mitsuya H**.	Structure-based design: synthesis and biological evaluation of a series of novel cycloamide-derived HIV-1 protease inhibitors.	***J Med Chem***	48	3576-3585	2005
Matsushita S, Yoshimura K, Kimura T, Kamihira A, Takano M, Eto K, Shirasaka T, **Mitsuya H**, and Oka S.	Spontaneous recovery of hemoglobin and neutrophil levels in Japanese patients on a long-term Combivir® containing regimen.	***J Clin Virol***	33	188-193	2005
Depboylu C, Schafer MK, Schwaeble WJ, Reinhart TA, Maeda H, **Mitsuya H**, Damadzic R, Rausch DM, Eiden LE, and Weihe E.	Increase of C1q biosynthesis in brain microglia and macrophages during lentivirus infection in the rhesus macaque is sensitive to antiretroviral treatment with 6-chloro-2',3'-dideoxyguanosine.	***Neurobiol Dis***	20	12-26	2005
Gatanaga H, Das D, Suzuki Y, Yeh DD, Hussain KA, Ghosh AK, and **Mitsuya H**.	Altered HIV-1 gag protein interactions with cyclophilin A (CypA) on the acquisition of H219Q and H219P substitutions in the CypA binding loop.	***J Biol Chem***	281	1241-1250	2006
Maeda K, Das D, Ogata-Aoki H, Nakata H, Miyakawa T, Tojo Y, Norman R, Takaoka Y, Ding J, Arnold E, and **Mitsuya H**.	Structural and molecular interactions of CCR5 inhibitors with CCR5.	***J Biol Chem*** Published on-lin on February 13, 2006.			2006

発表者氏名	論文タイトル名	発表誌名	巻号	ページ	出版年
Ghosh AK, Schiltz G, Perali RS, Leshchenko S, Kay S, Walters DE, Koh Y, Maeda K, and **Mitsuya H**.	Design and synthesis of novel HIV-1 protease inhibitors incorporating oxyindoles as the P'_2-ligands.	***Bioor Med Chem Let***	76	1869-1873	2006
Yin PD, Das D, and **Mitsuya H**.	Overcoming HIV Drug Resistance through Rational Drug Design Based on Molecular, Biochemical, and Structural Profiles of HIV Resistance.	***Cell Mol Life Sci*** (in the press)			

JOURNAL OF VIROLOGY, Feb. 2005, p. 2087–2096 Vol. 79, No. 4
0022-538X/05/$08.00+0 doi:10.1128/JVI.79.4.2087–2096.2005

Potent Anti-R5 Human Immunodeficiency Virus Type 1 Effects of a CCR5 Antagonist, AK602/ONO4128/GW873140, in a Novel Human Peripheral Blood Mononuclear Cell Nonobese Diabetic-SCID, Interleukin-2 Receptor γ-Chain-Knocked-Out AIDS Mouse Model

Hirotomo Nakata,[1] Kenji Maeda,[1] Toshikazu Miyakawa,[1] Shiro Shibayama,[2] Masayoshi Matsuo,[2] Yoshikazu Takaoka,[2] Mamoru Ito,[3] Yoshio Koyanagi,[4]† and Hiroaki Mitsuya[1,5]*

Department of Infectious Diseases, Kumamoto University Graduate School of Medicine, Kumamoto,[1] Ono Pharmaceutical Co. Ltd., Osaka,[2] Central Institute for Experimental Animals, Kawasaki,[3] Department of Virology, Tohoku University Graduate School of Medicine, Sendai,[4] Japan, and Experimental Retrovirology Section, HIV and AIDS Malignancy Branch, National Cancer Institute, Bethesda, Maryland[5]

Received 27 May 2004/Accepted 1 October 2004

We established human peripheral blood mononuclear cell (PBMC)-transplanted R5 human immunodeficiency virus type 1 isolate JR-FL (HIV-1_{JR-FL})-infected, nonobese diabetic-SCID, interleukin 2 receptor γ-chain-knocked-out (NOG) mice, in which massive and systemic HIV-1 infection occurred. The susceptibility of the implanted PBMC to the infectivity and cytopathic effect of R5 HIV-1 appeared to stem from hyperactivation of the PBMC, which rapidly proliferated and expressed high levels of CCR5. When a novel spirodiketopiperazine-containing CCR5 inhibitor, AK602/ONO4128/GW873140 (molecular weight, 614), was administered to the NOG mice 1 day after R5 HIV-1 inoculation, the replication and cytopathic effects of R5 HIV-1 were significantly suppressed. In saline-treated mice ($n = 7$), the mean human $CD4^+/CD8^+$ cell ratio was 0.1 on day 16 after inoculation, while levels in mice ($n = 8$) administered AK602 had a mean value of 0.92, comparable to levels in uninfected mice ($n = 7$). The mean number of HIV-RNA copies in plasma in saline-treated mice were $\sim 10^6$/ml on day 16, while levels in AK602-treated mice were 1.27×10^3/ml ($P = 0.001$). AK602 also significantly suppressed the number of proviral DNA copies and serum p24 levels ($P = 0.001$). These data suggest that the present NOG mouse system should serve as a small-animal AIDS model and warrant that AK602 be further developed as a potential therapeutic for HIV-1 infection.

Highly active antiretroviral therapy has brought about a major impact on the AIDS epidemics in the industrially advanced nations (5, 22). However, eradication of human immunodeficiency virus type 1 (HIV-1) is thought to be currently impossible, due in part to the viral reservoirs remaining in blood and infected tissues (6). The limitation of antiviral therapy of AIDS is exacerbated by complicated regimens, the development of drug-resistant HIV-1 variants (11), and a number of inherent adverse effects (2, 31). Hence, the identification of new antiretroviral drugs that have unique mechanisms of action and produce no or minimal adverse effects remains an important therapeutic objective. In regard to development of potential anti-HIV therapies or vaccines, experimental animal models for AIDS which allow the determination of the possible efficacy of antiviral agents or vaccines have been sought since severe combined immunodeficiency (SCID) mice engrafted with human fetal thymus, liver, or peripheral blood mononuclear cells (PBMC) were first exploited to examine antiretroviral agents (19, 25). However, a number of mouse models have suffered from false-positive and false-negative results in detecting or quantifying HIV-1 infection and replication and have required a large number of samples and mice for testing (25, 29).

In the present work, we established human PBMC-transplanted R5 HIV-1_{JR-FL}-infected, nonobese diabetic (NOD)-SCID, interleukin 2 receptor γ (IL-2Rγ)-chain-knocked-out (NOG) mice, in which massive and systemic HIV-1 infection occurs, human $CD4^+/CD8^+$ cell ratios significantly decrease, and high levels of R5 HIV-1 viremia reaching as high as 10^6 copies/ml are achieved. Furthermore, we demonstrated that this unprecedented susceptibility of the implanted human PBMC to the infectivity and cytopathic effects of R5 HIV-1 infection stems from hyperactivation of the PBMC. Here, we also report a novel small nonpeptide CCR5 antagonist, AK602/ONO4128/GW873140, which exerts potent anti-HIV-1 activity in vitro against laboratory and clinical strains of HIV-1, including highly multidrug-resistant (MDR) variants.

* Corresponding author. Mailing address: Department of Infectious Diseases, Kumamoto University Graduate School of Medicine, 1-1-1 Honjo, Kumamoto 860-8556, Japan. Phone: 81-96-373-5156. Fax: 81-96-363-5265. E-mail: hmitsuya@helix.nih.gov.

† Present address: Laboratory of Viral Pathogenesis, Institute for Virus Research, Kyoto University, Kyoto 606-8507, Japan.

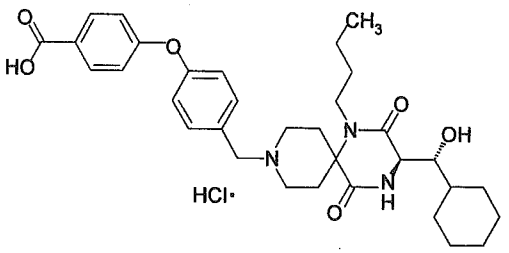

FIG. 1. Structure of AK602.

MATERIALS AND METHODS

Transplantation of human PBMC in NOG mice. NOD-SCID (NOG) mice (10, 33) were maintained in the Central Institute for Experimental Animals (Kawasaki, Japan). Mice were 4 to 6 weeks old at the time of transfer of human PBMC. The human PBMC-transplanted NOG (hu-PBMC-NOG)$_t$ mice were generated by methods previously described (23, 24). Briefly, PBMC (10^7) were freshly prepared from heparinized blood of a single healthy HIV-1-seronegative donor by Ficoll-Hypaque density gradient centrifugation, resuspended in RPMI 1640-based culture medium (0.5 ml), and infused intraperitoneally to each mouse. The experimental protocol was approved by the Ethics Review Committees for Animal Experimentation of the participating institutions.

Assay for proliferation and CCR5 expression of transplanted human PBMC recovered from hu-PBMC-NOG mice. Freshly isolated human PBMC (2×10^7 cells/ml) were incubated in phosphate-buffered saline (PBS) containing 10 μM 5-carboxyfluorescein diacetate succinimidyl ester (CFSE; Molecular Probes, Eugene, Oreg.) for 15 min at 37°C for CFSE labeling as previously described by Lyons (16), washed, and resuspended in RPMI 1640. One part of the labeled PBMC preparation was intraperitoneally injected (10^7 PBMC) to each NOG mouse, and human PBMC were recovered from peritoneal lavages and spleen. The other part of the preparation was immediately stimulated with 10 μg of phytohemagglutinin (PHA)/ml, cultured, and harvested. PBMC samples thus obtained were labeled with phycoerythrin (PE)-conjugated anti-CCR5 monoclonal antibody 3A9 or peridinin chlorophyll protein-conjugated anti-HLA-DR antibody (BD Pharmingen, San Diego, Calif.) and subjected to flow cytometric analysis with a Becton Dickinson FACscan cytometer; the data were analyzed by Cell Quest software (Becton Dickinson, Franklin Lakes, N.J.). A quantitative fluorescence-activated cell sorting (FACS) assay that relies on a series of precalibrated beads that bind to a fixed number of mouse immunoglobulin G molecules (Quantum Simply Cellular Kit; Sigma, Saint Louis, Mo.) to determine the absolute number of CCR5s on the cell surface was also conducted according to the manufacturer's instructions (15).

Cells and viruses. The HeLa-CD4-LTR-β-gal indicator cell line expressing human CCR5 (CCR5$^+$ MAGI) (18), a kind gift from Yosuke Maeda, was used for the present study. 293T cells (a human embryonic kidney cell line) were cultured in Dulbecco's modified Eagle medium supplemented with 10% fetal calf serum (FCS) and antibiotics and used for transfection of DNA plasmid containing the R5 HIV-$1_{JR\text{-}FL}$ genome (13). PBMC isolated from HIV-1-seronegative individuals were cultured with 10% FCS and antibiotics with 10 μg of PHA/ml for 3 days prior to anti-HIV-1 activity assay in vitro (PHA-PBMC). A panel of HIV-1 strains was employed for the drug susceptibility attempt: HIV-$1_{Ba\text{-}L}$ (7), HIV-$1_{JR\text{-}FL}$ (13), HIV-$1_{NL4\text{-}3}$ (32), a wild-type HIV-1_{MOKW} isolated from a drug-naive AIDS patient (17), and MDR primary HIV-1 (HIV-1_{MDR}) strain (HIV-1_{JSL} and HIV-1_{MM}) (35). All primary HIV-1 strains were passaged once or twice in PHA-PBMC cultures and the culture supernatants were stored at −80°C until use. Antiviral assays using PHA-PBMC were conducted as previously reported (12, 17, 35).

Antiviral agents and assay for inhibition of R5 HIV-1 infectivity and replication. A series of different spirodiketopiperazine (SDP) derivatives were newly designed, synthesized, and tested for their activity against in vitro infectivity and replication of R5 HIV-1 as previously described (17). AK602 was chosen for this study based on its CCR5-specific, potent activity against R5 HIV-1. A method for the synthesis of AK602 will be published elsewhere. The structure of AK602 is illustrated in Fig. 1. An approved drug for therapy for HIV-1 infection, 2′,3′-dideoxyinosine (ddI) (20, 21), was kindly provided by Ajinomoto Co., Inc, Tokyo, Japan. TAK779 and SCH-C were synthesized according to previously published data (1, 30). The MAGI assay using CCR5$^+$ MAGI cells was conducted as previously described (17) with minor modifications. Briefly, CCR5$^+$ MAGI cells were seeded in 96-well, flat-bottomed microculture plates (10^4 cells/well) for 24 h, exposed to 0.1 or 1 μM AK602 for 30 min, washed three times, exposed to R5 HIV-1 (100 50% tissue culture infectious doses) at various time points after AK602 removal, and cultured in Dulbecco's modified Eagle medium containing 15% FCS for 48 h. Following the removal of supernatants and lysis of the cells with PBS (100 μl) containing 1% Triton X-100, a solution (100 μl) containing 10 mM chlorophenol red-β-D-galactopyranoside, 2 mM $MgCl_2$, and 0.1 M KH_2PO_4 was added to each well; the mixture was incubated at room temperature in the dark for 30 min; and the optical density (wavelength, 570 nm) was measured with a microplate reader (*V*max, Molecular Devices, Sunnyvale, Calif). All assays were performed in triplicate.

Pharmacokinetic analysis of AK602 in hu-PBMC-NOG mice. Pharmacokinetic analysis of AK602 in hu-PBMC-NOG mice was performed as previously described (28). In brief, plasma samples were collected periodically over 12 h, following a single AK602 administration at a dose of 60 mg/kg of body weight dissolved in 400 μl of 4% hydroxypropyl-β cyclodextrin (HPBC). Each plasma sample (150 μl) was centrifuged at 3,000 rpm for 10 min, and the supernatant was vacuum concentrated and injected into the high-performance liquid chromatography (HPLC) system. The eluent was monitored at 255 nm of UV, and the AK602 concentration in plasma was determined.

Determination of amounts of AK602 persistently bound to CCR5 in hu-PBMC-NOG mice. Blood samples were collected from the tail vein of each hu-PBMC-NOG mouse at various time points following a single intraperitoneal administration of AK602 at a dose of 60 mg/kg. PBMC were isolated by density gradient centrifugation and stained with fluorescein isothiocyanate-conjugated monoclonal antibody 45531 (R&D Systems, Minneapolis, Minn.) specific for the C-terminal half of the second extracellular loop (ECL2B) of CCR5 (15) known to be competitively replaced by SDP derivatives (17) or with PE-conjugated monoclonal antibody 3A9, which binds to the N-terminus extracellular domain of CCR5 (17). PBMC were then subjected to FACS analysis.

Treatment of R5 HIV-1-infected hu-PBMC-NOG mice with anti-HIV-1 agents. Sixteen days after PBMC infusion, the mice were bled from the tail vein, and three-color flow cytometric analysis was performed to confirm positive engraftment of human HLA, CD4, and CD8 antigens on the cells recovered. HIV-$1_{JR\text{-}FL}$ (2,000 50% tissue culture infectious doses) was intraperitoneally inoculated to each mouse in which PBMC engraftment was confirmed. Twenty-four hours after the R5 HIV-1 inoculation, administration of AK602 (120 mg in 4% HPBC/kg/day, twice a day), ddI (50 mg in 4% HPBC/kg/day, twice a day), or saline was implemented and continued by day 16. On days 5 and 9 after the R5 HIV-1 inoculation, blood samples were collected from mouse tail veins for immunologic and virological monitoring (see below). On day 16, blood samples were collected by cardiocentesis, and the mice were sacrificed. The experimental protocol for the treatment is illustrated in Fig. 2.

Immunologic and virological monitoring. Human PBMC recovered from mice were subjected to immunologic and virological monitoring as previously described (23, 24). The CD4$^+$/CD8$^+$ cell ratios were determined by FACS analysis with PE-conjugated mouse anti-CD4 and peridinin chlorophyll protein-conjugated mouse anti-CD8 (BD Pharmingen) monoclonal antibodies. Determination of HIV-1 DNA copy numbers in recovered human PBMC was performed by real-time PCR assay with Taqman Master mixture (PE Biosystems) and HIV long terminal repeat-specific primers M667 (5′-GGC TAA CTA GGG AAC CCA CTG-3′) and AA55 (5′-CTG CTA GAG ATT TTC CAC ACT GAC-3′). HIV-1-specific products were quantified with the ABI 7700 detection system (Applied Biosystems, Foster City, Calif.), and cell numbers were determined with the RAG-1 gene. The numbers of CD4$^+$ cells were calculated based on the percentage of CD4$^+$ values obtained from the FACS analysis of each test PBMC sample, and R5 HIV-1 proviral DNA copy numbers were expressed as copy numbers per 10^5 CD4$^+$ cells. In some experiments, CD4$^+$ and CD4$^-$ cells were separated before real-time PCR assay with the rapid immunomagnetic CD4-positive cell isolation kit (Dynabeads M-450 CD4; Dynal Biotech, Inc., Lake

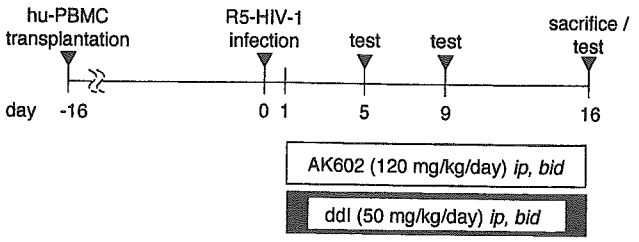

FIG. 2. Protocol for drug administration and immunological and virologic monitoring.

Success, N.Y.). The amounts of p24 antigen in murine sera were determined using a fully automated chemiluminescent enzyme immunoassay system (Lumipulse F; Fujirebio, Inc., Tokyo, Japan) as previously described (12). Plasma viral load was quantified with the AMPLICOR HIV-1 monitor test kit, version 1.5 (Roche Diagnostics, Branchburg, N.J.).

Statistical analyses. Nonparametric statistical analyses were performed by using the Mann-Whitney U test (Statview, version 5.0; Abacus Concepts, Berkeley, Calif.). The difference between viremia levels in two groups of mice was determined by the Wilcoxon rank sum test. For each mouse, the value of $\log_{10}$ RNA copies was calculated, and the slope corresponding to the rate of increase per day was determined by simple linear regression for the days (5, 9, and 16) of blood collection. The resulting slopes for all mice in the untreated groups were compared to the slopes of mice in each of the other two groups.

RESULTS

Transplanted PBMC in hu-PBMC-NOG mice are intensely activated and express high levels of CCR5. When we examined the proliferation profile of PBMC stimulated with PHA in vitro by treatment with the vital dye CFSE, which allows the analysis of cell proliferation as the CFSE's fluorescence intensity is halved per each cell division, there was only a slight shift to the left in the flow cytometric profile on days 1 and 2 of culture (Fig. 3A). On day 4 of culture, a discrete shift to the left was identified, suggesting that the PHA-PBMC underwent up to four cycles of proliferation in vitro by day 4. In contrast, PBMC transplanted and recovered on day 2 had apparently undergone ~4 cycles of proliferation; by day 4, a majority of cells had undergone up to 10 cycles and beyond in proliferation (Fig. 3B). It was possible that the CFSE-negative and weakly CFSE-positive cells which accumulated on days 2 and 4 (Fig. 3B) were murine cells that engulfed and degraded CFSE. We therefore conducted experiments in which the cells with CFSE dilution were directly confirmed to be human CCR5-positive cells. As can be seen in Fig. 3C, when cells were recovered from the spleen of an NOG mouse into which CFSE-labeled PBMC had been transplanted and stained with monoclonal antibody 45531, which is specific for the C-terminal half of the second extracellular loop (ECL2B) of CCR5 (15), the majority of such human $CCR5^+$ cells proved to be CFSE negative. We also examined the levels of cellular activation by the expression of HLA-DR on cell surface. The levels of HLA-DR expression in PBMC recovered from uninfected NOG mice 3 days after transplantation were much greater than those in 3-day-cultured PBMC following PHA stimulation (Fig. 3D). The fluorescence intensity in the same donor's PHA-PBMC examined on three different occasions was 21 ± 4, while that of the PBMC recovered from mice was 91 ± 25 (Fig. 3D). When we further assessed the levels of CCR5 expression, the PBMC recovered from the mice on day 3 proved to be strongly positive for CCR5 (Fig. 3E). The CCR5-positive fraction in the PBMC recovered was 49.7%, while that in PHA-PBMC was 27.3%. The mean fluorescence intensity of the $CCR5^+$ cell population was 141, compared to the $CCR5^+$ cell population in PHA-PBMC with a mean fluorescence intensity of 51. The estimated number of CCR5 expressed on the PBMC recovered on day 3 was 25,348 (as antibody binding sites per cell) while that on PHA-PBMC on day 3 in culture was 8,981 antibody binding sites as examined by quantitative FACS assay. These data indicate that the transplanted human PBMC were intensely activated and rapidly proliferating and expressed high levels of CCR5 on their cell surfaces.

Potent activity of AK602 against R5 HIV-1 in vitro. Among SDP derivatives we designed and synthesized, AK602 was identified to be highly potent against a broad spectrum of R5 HIV-1 strains, including MDR clinical R5 HIV-1 isolates in vitro with 50% inhibitory concentration (IC_{50}) values of 0.3 to 0.6 nM, although two previously published CCR5 antagonists (TAK779 and SCH-C) were substantially less potent than AK602 (Table 1). AK602 and other CCR5 antagonists failed to inhibit the replication of an X4 HIV-1 strain, HIV-1_{NL4-3}.

Pharmacokinetics of AK602 in hu-PBMC-NOG mice. We examined the pharmacokinetics of AK602 in hu-PBMC-NOG mice by intraperitoneally administering the compound at a dose of 60 mg/kg. Plasma samples were collected periodically up to 12 h and subjected to HPLC analysis. As shown in Fig. 4A, the concentration of AK602 reached the maximal concentration immediately after intraperitoneal administration and decreased rapidly. The calculated plasma half-life in the α-phase of the concentration curve was as short as 29 min.

AK602 persists on cell surface CCR5. As shown above, the plasma half-life of AK602 turned out to be short; however, considering that AK602 possesses such a high affinity to CCR5 and potent activity against R5 HIV-1 in vitro, it was thought possible that AK602 would remain attached on cellular CCR5 for an extensive period of time and exert anti-R5 HIV-1 activity even when the compound was depleted from circulation. To examine this possibility, we used two monoclonal antibodies, 45531 and 3A9. When human PBMC were recovered from a hu-PBMC-NOG mouse 2 and 6 h after AK602 administration (60 mg/kg) and stained with 45531, AK602 proved to block the binding of 45531 to CCR5 (Fig. 4B), while AK602 failed to block 3A9 binding to CCR5 (Fig. 4C), suggesting that AK602 did not elicit CCR5 internalization or shedding at all at least for 6 h. We subsequently examined whether AK602 remained on cellular CCR5 with the 45531 monoclonal antibody. When the cells were recovered from mice 2, 6, and 14 h after the AK602 administration, the mean values of the percentage of AK602 occupancy were 85 (four mice), 54 (three mice), and 16 (three mice), respectively. It was calculated that it took about 9 h for AK602 occupancy to be reduced by 50% (Fig. 4D).

Anti-R5 HIV-1 activity of AK602 persistently seen after its removal from culture medium. In another depletion experiment, we exposed $CCR5^+$ MAGI cells to AK602 for 30 min, depleted the compound from the culture by thorough washing, incubated the cells for various lengths of time, exposed the cells to HIV-1_{Ba-L}, further cultured the cells for 48 h, and determined whether HIV-1_{Ba-L} infection was blocked by AK602 exposure (Fig. 4E). When the $CCR5^+$ MAGI cells were exposed to 0.1 and 1 μM AK602 and exposed to HIV-1_{Ba-L} immediately afterward, the values for protection were 68 and 85%, respectively. When the cells were exposed to HIV-1_{Ba-L} 4 h after depletion, 49 and 72% of the cells were protected by 0.1 and 1 μM AK602. When the cells were exposed to HIV-1_{Ba-L} 12 and 24 h after depletion, 57 and 45% of the cells were seen protected by 1 μM, respectively (Fig. 4E).

Effects of AK602 on $CD4^+$ and $CD8^+$ cell counts in R5 HIV-1-infected hu-PBMC-NOG mice. PBMC were recovered from murine blood samples collected on days 5, 9, and 16 after R5 HIV-1 inoculation and subjected to flow cytometric analysis for determination of $CD4^+/CD8^+$ cell ratios. As shown in Fig. 5A, in PBMC recovered on day 16 from a representative

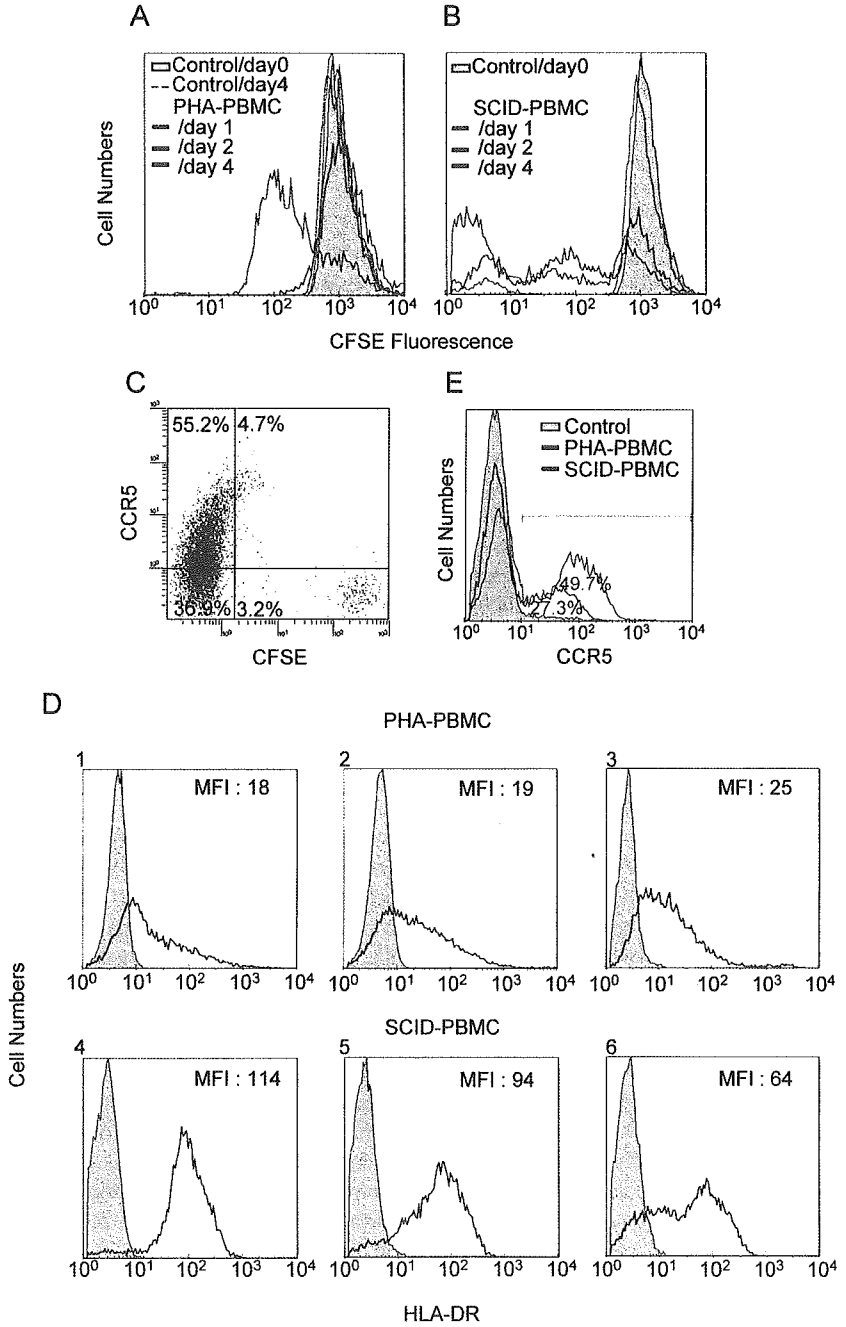

FIG. 3. Transplanted PBMC are intensely activated and express high levels of CCR5. (A and B) Proliferation profiles of PHA-PBMC and transplanted and recovered PBMC. Freshly prepared PBMC were incubated with the vital dye CFSE, and one part of such PBMC preparation was stimulated with PHA, while the other part was intraperitoneally transplanted to mice. On days 1, 2, and 4, the cells were harvested and the fluorescence intensity of CFSE was determined. Note that transplanted PBMC recovered on day 2 had undergone ~4 cycles of proliferation; by day 4, a majority of cells had undergone ~10 cycles and more of proliferation. (C) CCR5 expression level and CFSE intensity in human PBMC harvested from a spleen of hu-PBMC-NOG mouse on day 4. (D) Intense activation of PBMC after transplantation. PBMC stimulated with PHA and cultured for 4 days (panels 1 to 3) and transplanted PBMC recovered from the uninfected mice on day 4 (panels 4 to 6) were stained with an anti-HLA-DR monoclonal antibody. Note that HLA-DR expression levels in transplanted PBMC were much higher than those in PHA-PBMC. (E) CCR5 expression profiles of PHA-PBMC and transplanted PBMC. PBMC stimulated with PHA and cultured for 3 days and transplanted PBMC recovered from the uninfected mice on day 3 were stained with PE-conjugated anti-CCR5 monoclonal antibody 3A9 and subjected to flow cytometric analysis. SCID-PBMC, PBMC transplanted and recovered.

R5 HIV-1-infected, saline-treated mouse, there were only few $CD4^+$ cells (3.9% [1.4% + 2.5%]) resulting in a $CD4^+/CD8^+$ cell ratio of 0.05. However, a distinct $CD4^+$ cell population (55.1% [4.4% + 50.7%]) resulting in a $CD4^+/CD8^+$ ratio of 1.84 (Fig. 5B) was seen in PBMC recovered from an AK602-treated mouse, and the size of this $CD4^+$ cell population was comparable to that seen in a ddI-treated mouse (53.2% [3.8% + 49.4%]) and that in an uninfected mouse (48.9% [3.8% +